glucuronide to morphine 6-*O*-glucuronide in liver microsomes of mice, rats, guinea pigs, and rabbits were 300:1, 90:1, 4:1, and 40:1, respectively (Kuo et al., 1991). The formation of morphine 3-*O*-glucuronide is catalyzed by human UGT2B7 (Turgeon et al., 2001) and rat UGT2B1 (King et al., 2000). However, there is no information on the mouse Ugt enzyme that catalyzes morphine 3-*O*-glucuronidation. Rat UGT2B1 and mouse Ugt2b1 are predominantly expressed in the liver (Shelby et al., 2003; Buckley and Klaassen, 2007). In the present study, the morphine 3-*O*-glucuronidation was higher in the liver, compared with intestine, in both mice and rats as well as humans (Fisher et al., 2000b). The indication is that the glucuronidation of morphine in mice may occur mainly in liver as in rats and humans. In addition, in the present study, there were no sex differences in morphine 3-*O*-glucuronidation in either mice or rats, consistent with a report on the sex differences in morphine glucuronidation in vivo and in vitro (Rush et al., 1983). However, in the case of bisphenol A glucuronidation catalyzed by rat UGT2B1, the ratio of bisphenol A glucuronide to total bisphenol A in liver microsomes was significantly higher ($P = 0.015$) in female than in male Wistar-Imamichi rats, and the relative hepatic expression level of UGT2B1 mRNA was significantly higher ($P < 0.001$) in female than in male rats (Takeuchi et al., 2004). Therefore, when morphine 3-*O*-glucuronidation in rat liver is evaluated, the involvement of other UGTs as well as UGT2B1 may need to be considered.

TFP is a specific probe substrate for human UGT1A4 (Uchaipichat et al., 2006). However, rat *UGT1A4* and mouse *Ugt1a4* are known to be pseudogenes. In the present study, TFP *N*-glucuronidation in mice and rats could not be detected. Therefore, we should be careful in studies of drugs catalyzed by UGT1A4.

In the present study, the UGT activities in mouse and rat duodenum, jejunum, ileum, and colon were determined. The UGT activities in rats tended to decrease from duodenum to ileum, whereas this tendency in mice differed according to the substrates. These phenomena may be due to the expression levels of UGT or to the function of the UGT, but further study is needed. Strassburg et al. (2000) reported that the UGT activities in human intestine were higher in the jejunum than in duodenum or ileum. The present study clarified that this tendency in intestine may be different among mice, rats, and humans.

There are few reports concerning strain differences in UGT activities in mice. The UGT activities of five different substrates, except for 4-MU, showed the highest activities in C3H/HeJ mice. In contrast, the glucuronidation in DBA/2 mice was relatively low compared with that in the other strains. The strain differences in estradiol 3-*O*-, 4-NP *O*-, propofol *O*-, and MPA *O*-glucuronidation were similar. Why such strain differences were observed is not known exactly.

In conclusion, the present study clarified the fact that species differences exist between rats and mice in terms of their duodenal and hepatic UGT activities. The species, strain, and sex differences may depend on the substrate or UGT enzyme. The present study will provide useful information for the selection of species for in vivo UGT studies. Furthermore, experimental animals are useful tools for the development of new drugs, and thus studies on species differences are of great value for extrapolating results from animals to humans. The present study will also provide useful information for predicting drug metabolism catalyzed by UGTs.

References

Bernard O and Guillemette C (2004) The main role of UGT1A9 in the hepatic metabolism of mycophenolic acid and the effects of naturally occurring variants. *Drug Metab Dispos* **32:**775–778.

Buckley DB and Klaassen CD (2007) Tissue- and gender-specific mRNA expression of UDP-glucuronosyltransferases (UGTs) in mice. *Drug Metab Dispos* **35:**121–127.

Burchell B, Soars M, Monaghan G, Cassidy A, Smith D, and Ethell B (2000) Drug-mediated toxicity caused by genetic deficiency of UDP-glucuronosyltransferases. *Toxicol Lett* **112–113:** 333–340.

Coffman BL, King CD, Rios GR, and Tephly TR (1998) The glucuronidation of opioids, other xenobiotics, and androgens by human UGT2B7Y(268) and UGT2B7H(268). *Drug Metab Dispos* **26:**73–77.

Court MH (2001) Acetaminophen UDP-glucuronosyltransferase in ferrets: species and gender differences, and sequence analysis of ferret UGT1A6. *J Vet Pharmacol Ther* **24:**415–422.

Court MH (2005) Isoform-selective probe substrates for in vitro studies of human UDP-glucuronosyltransferases. *Methods Enzymol* **400:**104–116.

Dutton GJ (1980) Acceptor substrates of UDP glucuronosyltransferase and their assay, in *Glucuronidation of Drugs and Other Compounds* (Dutton GJ ed) pp 69–78, CRC Press, Boca Raton, FL.

Emoto C, Yamazaki H, Shimada N, Nakajima M, and Yokoi T (2000) Characterization of cytochrome P450 enzyme involved in drug oxidations in mouse intestinal microsomes. *Xenobiotica* **10:**943–953.

Fisher MB, Campanale K, Ackermann BL, VandenBranden M, and Wrighton SA (2000a) In vitro glucuronidation using human liver microsomes and the pore-forming peptide alamethicin. *Drug Metab Dispos* **28:**560–566.

Fisher MB, Vandenbranden M, Findlay K, Burchell B, Thummel KE, Hall SD, and Wrighton SA (2000b) Tissue distribution and interindividual variation in human UDP-glucuronosyltransferase activity: relationship between UGT1A1 promoter genotype and variability in a liver bank. *Pharmacogenetics* **10:**727–739.

Fujiwara R, Nakajima M, Yamanaka H, Nakamura A, Katoh M, Ikushiro S, Sakaki T, and Yokoi T (2007) Effects of coexpression of UGT1A9 on enzymatic activities of human UGT1A isoforms. *Drug Metab Dispos* **35:**747–757.

Hanioka N, Jinno H, Tanaka-Kagawa T, Nishimura T, and Ando M (2001) Determination of UDP-glucuronosyltransferase UGT1A6 activity in human and rat liver microsomes by HPLC with UV detection. *J Pharm Biomed Anal* **25:**65–75.

Hanioka N, Takeda Y, Jinno H, Tanaka-Kagawa T, Naito S, Koeda A, Shimizu T, Nomura M, and Narimatsu S (2006) Functional characterization of human and cynomolgus monkey UDP-glucuronosyltransferase 1A6 enzymes. *Chem Biol Interact* **164:**136–145.

Harding D, Fournel-Gigleux S, Jackson MR, and Burchell B (1988) Cloning and substrate specificity of a human phenol UDP-glucuronosyltransferase expressed in COS-7 cells. *Proc Natl Acad Sci U S A* **85:**8381–8385.

Houston JB and Kenworthy KE (2000) In vitro-in vivo scaling of CYP kinetic data not consistent with the classical Michaelis-Menten model. *Drug Metab Dispos* **28:**246–254.

Iyanagi T, Haniu M, Sogawa K, Fujii-Kuriyama Y, Watanabe S, Shively JE, and Anan KF (1986) Cloning and characterization of cDNA encoding 3-methylcholanthrene inducible rat mRNA for UDP-glucuronosyltransferase. *J Biol Chem* **261:**15607–15614.

Katoh M, Matsui T, Okumura H, Nakajima M, Nishimura M, Naito S, Tateno C, Yoshizato K, and Yokoi T (2005) Expression of human phase II enzymes in chimeric mice with humanized liver. *Drug Metab Dispos* **33:**1333–1340.

King C, Finley B, and Franklin R (2000) The glucuronidation of morphine by dog liver microsomes: identification of morphine-6-*O*-glucuronide. *Drug Metab Dispos* **28:**661–663.

King CD, Green MD, Rios GR, Coffman BL, Owens IS, Bishop WP, and Tephly TR (1996) The glucuronidation of exogenous and endogenous compounds by stably expressed rat and human UDP-glucuronosyltransferase 1.1. *Arch Biochem Biophys* **332:**92–100.

Krishnaswamy S, Duan SX, Von Moltke LL, Greenblatt DJ, Sudmeier JL, Bachovchin WW, and Court MH (2003) Serotonin (5-hydroxytryptamine) glucuronidation in vitro: assay development, human liver microsome activities and species differences. *Xenobiotica* **33:**169–180.

Kuo CK, Hanioka N, Hoshikawa Y, Oguri K, and Yoshimura H (1991) Species difference of site-selective glucuronidation of morphine. *J Pharmacobiodyn* **14:**187–193.

Lamb JG, Straub P, and Tukey RH (1994) Cloning and characterization of cDNAs encoding mouse Ugt1.6 and rabbit UGT1.6: differential induction by 2,3,7,8-tetrachlorodibenzo-*p*-dioxin. *Biochemistry* **33:**10513–10520.

Lowry OH, Rosebrough NJ, Farr AL, and Randall RJ (1951) Protein measurement with the Folin phenol reagent. *J Biol Chem* **193:**265–275.

Mackenzie PI, Bock KW, Burchell B, Guillemette C, Ikushiro S, Iyanagi T, Miners JO, Owens IS, and Nebert DW (2005) Nomenclature update for the mammalian UDP glycosyltransferase (*UGT*) gene superfamily. *Pharmacogenet Genomics* **15:**677–685.

Mano Y, Usui T, and Kamimura H (2004) Effects of β-estradiol and propofol on the 4-methylumbelliferone glucuronidation in recombinant human UGT isozymes 1A1, 1A8 and 1A9. *Biopharm Drug Dispos* **25:**339–344.

Miles KK, Kessler FK, Smith PC, and Ritter JK (2006) Characterization of rat intestinal microsomal UDP-glucuronosyltransferase activity toward mycophenolic acid. *Drug Metab Dispos* **34:**1632–1639.

Miles KK, Stern ST, Smith PC, Kessler FK, Ali S, and Ritter JK (2005) An investigation of human and rat liver microsomal mycophenolic acid glucuronidation: evidence for a principal role of UGT1A enzymes and species differences in UGT1A specificity. *Drug Metab Dispos* **33:**1513–1520.

Milne RW, Nation RL, and Somogyi AA (1996) The disposition of morphine and its 3- and 6-glucuronide metabolites in humans and animals, and the importance of the metabolites to the pharmacological effects of morphine. *Drug Metab Rev* **28:**345–472.

Miners JO, Lillywhite KJ, Matthews AP, Jones ME, and Birkett DJ (1988) Kinetic and inhibitor studies of 4-methylumbelliferone and 1-naphthol glucuronidation in human liver microsomes. *Biochem Pharmacol* **37:**665–671.

Muraca M and Fevery J (1984) Influence of sex and sex steroids on bilirubin uridine diphosphate-glucuronosyltransferase activity of rat liver. *Gastroenterology* **87:**308–313.

Picard N, Ratanasavanh D, Prémaud A, Le Meur Y, and Marquet P (2005) Identification of the UDP-glucuronosyltransferase isoforms involved in mycophenolic acid phase II metabolism. *Drug Metab Dispos* **33:**139–146.

Rush GF, Newton JF, and Hook JB (1983) Sex differences in the excretion of glucuronide conjugates: the role of intrarenal glucuronidation. *J Pharmacol Exp Ther* **227:**658–662.

Shelby MK, Cherrington NJ, Vansell NR, and Klaassen CD (2003) Tissue mRNA expression of the rat UDP-glucuronosyltransferase gene family. *Drug Metab Dispos* **31:**326–333.

Sneyd JR, Simons PJ, and Wright B (1994) Use of proton NMR spectroscopy to measure propofol metabolites in the urine of the female Caucasian patient. *Xenobiotica* **24:**1021–1028.

Stern ST, Tallman MN, Miles KK, Ritter JK, Dupuis RE, and Smith PC (2007) Gender-related differences in mycophenolate mofetil-induced gastrointestinal toxicity in rats. *Drug Metab Dispos* **35:**449–454.

Strassburg CP, Kneip S, Topp J, Obermayer-Straub P, Barut A, Tukey RH, and Manns MP (2000) Polymorphic gene regulation and interindividual variation of UDP-glucuronosyltransferase activity in human small intestine. *J Biol Chem* **275:**36164–36171.

Takeuchi T, Tsutsumi O, Nakamura N, Ikezuki Y, Takai Y, Yano T, and Taketani Y (2004) Gender difference in serum bisphenol A levels may be caused by liver UDP-glucuronosyltransferase activity in rats. *Biochem Biophys Res Commun* **325:**549–554.

Tukey RH and Strassburg CP (2000) Human UDP-glucuronosyltransferases: metabolism, expression and disease. *Annu Rev Pharmacol Toxicol* **40:**581–616.

Turgeon D, Carrier JS, Lévesque E, Hum DW, and Belanger A (2001) Relative enzymatic activity, protein stability and tissue distribution of human steroid-metabolizing UGT2B subfamily members. *Endocrinology* **142:**778–787.

Uchaipichat V, Mackenzie PI, Elliot DJ, and Miners JO (2006) Selectivity of substrate (trifluoperazine) and inhibitor (amitriptyline, androsterone, canrenoic acid, hecogenin, phenylbutazone, quinidine, quinine, and sulfinpyrazone) "probes" for human UDP-glucuronosyltransferases. *Drug Metab Dispos* **34:**449–456.

Uchaipichat V, Mackenzie PI, Guo XH, Gardner-Stephen D, Galetin A, Houston JB, and Miners JO (2004) Human UDP-glucuronosyltransferases: isoform selectivity and kinetics of 4-methylumbelliferone and 1-naphthol glucuronidation, effects of organic solvents, and inhibition by diclofenac and probenecid. *Drug Metab Dispos* **32:**413–423.

Wen Z, Martin DE, Bullock P, Lee KH, and Smith PC (2007) Glucuronidation of anti-HIV drug candidate bevirimat: identification of human UDP-glucuronosyltransferases and species differences. *Drug Metab Dispos* **35:**440–448.

Yoon Y, Westerhoff P, Snyder SA, and Esparza M (2003) HPLC-fluorescence detection and adsorption of bisphenol A, 17β-estradiol, and 17α-ethynyl estradiol on powdered activated carbon. *Water Res* **37:**3530–3537.

Address correspondence to: Dr. Tsuyoshi Yokoi, Drug Metabolism and Toxicology, Division of Pharmaceutical Sciences, Graduate School of Medical Science, Kanazawa University, Kakuma-machi, Kanazawa 920-1192, Japan. E-mail: tyokoi@kenroku.kanazawa-u.ac.jp

210

Species Differences in UDP-Glucuronosyltransferase Activities in Mice and Rats

Hirotada Shiratani, Miki Katoh, Miki Nakajima, and Tsuyoshi Yokoi

Drug Metabolism and Toxicology, Division of Pharmaceutical Sciences, Graduate School of Medical Science, Kanazawa University, Kanazawa, Japan

ABSTRACT:

UDP-glucuronosyltransferases (UGTs), expressed in various tissues including liver and intestine, catalyze phase II metabolic biotransformation. There is little information on species differences between mice and rats in UGT activities, especially in intestine. The purpose of the present study was to clarify the species differences between mice and rats in UGT activities using duodenal and liver microsomes. For estradiol 3-O-glucuronidation in duodenal microsomes, the kinetic data in mice were fit to the Hill equation. However, the Hill coefficient was low in rats ($n = 1.1$), suggesting that rat estradiol 3-O-glucuronidation followed the Michaelis-Menten equation rather than the Hill equation. For 4-nitrophenol (4-NP) O-glucuronidation, the K_m values were different between mice and rats. The intrinsic clearance (CL_{int}) values for mycophenolic acid (MPA) O- and morphine 3-O-glucuronidation in male mouse duodenum were 3- and 17-fold lower than those in rat, respectively. In male liver, the CL_{int} values for 4-NP O-, propofol O-, MPA O-, and morphine 3-O-glucuronidation and the CL_{max} value for 4-methylumbelliferone O-glucuronidation in mice were higher than those in rats. The CL_{max} value for estradiol 3-O-glucuronidation in mice was lower than that in rats. Also, there were strain differences among C57BL/6J, BALB/c, C3H/HeJ, DBA/2, ddY, and ICR mice in UGT activities in duodenum. We clarified that the species differences in UGT activity evaluated by the CL_{int} or CL_{max} values in liver and duodenum varied according to the substrate.

UDP-glucuronosyltransferase (UGT) expressed in various tissues including liver and intestine catalyzes phase II metabolic biotransformation. UGTs conjugate lipophilic compounds with glucuronic acid from UDP-glucuronic acid (UDPGA), thereby increasing hydrophilicity and enhancing excretion through bile and urine (Dutton, 1980). In both humans and rodents, two families of UGT, UGT1 and UGT2, are known. The human *UGT1* gene contains 13 individual promoter/first exons and shares exons 2 to 5 (Mackenzie et al., 2005). As with the human genes, rat and mouse *Ugt1* genes also share exons 2 to 5 and have 10 and 14 first exons, respectively (Mackenzie et al., 2005). Among species, the numbers of the first exons and pseudogenes differ. There are four, two, and five pseudogenes in human, rat, and mouse UGT enzymes, respectively. For example, human *UGT1A4* is functional but rat *UGT1A4* and mouse *Ugt1a4* are pseudogenes. Human *UGT1A9* and mouse *Ugt1a9* are functional, but rat *UGT1A9* is a pseudogene. In the case of *UGT1A6*, mice have two functional copies of *Ugt1a6*, *Ugt1a6a* and *Ugt1a6b*, whereas humans and rats have one copy of *UGT1A6*. On the other hand, the *UGT2* gene in humans, rats, and mice consists of six exons, except for *UGT2A1* and *UGT2A2* genes (seven exons). The UGT2 family contains three enzymes of the UGT2A subfamily and seven enzymes of the UGT2B subfamily among humans, rats, and mice. The UGT2 subfamily shares more than 70% sequence homology, thus orthologs across species are

hard to elucidate (Mackenzie et al., 2005). These species differences in UGT genes could result in species differences in UGT activities.

Liver and intestine are the important tissues for drug metabolism including glucuronidation. The expression of UGT mRNAs has been reported in various tissues in humans (Tukey and Strassburg, 2000), rats (Shelby et al., 2003), and mice (Buckley and Klaassen, 2007). Comparison of expression levels among UGT enzymes is difficult. Because UGT antibodies are not available for the specific quantification of each UGT enzyme, the expression ratio of each UGT enzyme remains unclear in the liver and intestine. Which UGT enzyme in mice and rats corresponds to human UGT enzyme is controversial.

The UGT substrates include many endogenous and xenobiotic compounds. Typical endogenous substrates are bilirubin and estradiol. In particular, hyperbilirubinemia caused by a *UGT* defect is well known (Burchell et al., 2000). Small xenobiotic planar phenols such as 4-methylumbelliferone (4-MU) and 4-nitrophenol (4-NP) are often used for measuring the glucuronidation (Hanioka et al., 2006). Propofol, widely used as an intravenous anesthetic for the induction and maintenance of anesthesia, is metabolized mainly to its glucuronide in humans (Sneyd et al., 1994). A prodrug of mycophenolic acid (MPA), mycophenolate mofetil (MMF), exhibited severe gastrointestinal toxicity and a relationship between its toxicity and MPA glucuronidation is suspected in rats (Stern et al., 2007). Morphine, an analgesic drug used for the treatment of acute and chronic pain syndromes in cancer patients, is glucuronidated mainly by UGT2B7 in a stereoselective manner to morphine 3-O- and 6-O-glucuronide in humans (Coffman et al., 1998), whereas the main metabolite in humans and rodents is

---

ABBREVIATIONS: UGT/Ugt, UDP-glucuronosyltransferase; UDPGA, UDP-glucuronic acid; 4-MU, 4-methylumbelliferone; 4-NP, 4-nitrophenol; MPA, mycophenolic acid; MMF, mycophenolate mofetil; TFP, trifluoperazine.

3-O-glucuronide. Trifluoperazine (TFP), which is one of the antis-chizophrenic agents, is metabolized as N-glucuronide by human UGT1A4 (Uchaipichat et al., 2006).

In drug development, experimental animals are frequently used for pharmacokinetic studies. The investigation of species differences in drug metabolism is essential for understanding the results of in vivo animal studies. However, there is insufficient information on species differences in glucuronidation. The purpose of the present study was to clarify the species differences in mouse and rat UGT activities in intestine and liver using seven typical substrates (estradiol, 4-MU, 4-NP, MPA, propofol, morphine, and TFP).

Materials and Methods

Materials. UDPGA, alamethicin, aprotinin, bestatin, leupeptin, trypsin inhibitor (type II-S: soybean), estradiol, estradiol 3-O-glucuronide, 4-MU, 4-MU O-glucuronide, and 4-NP O-glucuronide were purchased from Sigma-Aldrich (St. Louis, MO). (p-Amidinophenyl)methanesulfonyl fluoride, MPA, 4-NP, and TFP were obtained from Wako Pure Chemicals (Osaka, Japan). Morphine hydrochloride was purchased from Takeda Pharmaceutical Company (Osaka, Japan). Morphine 3-O-glucuronide was kindly provided by Dr. Kazuta Oguri (Kyusyu University, Fukuoka, Japan). MPA O-glucuronide and carboxybutoxy ether of mycophenolic acid were generous gifts from Roche Bioscience (Palo Alto, CA). All other chemicals and solvents were of analytical grade or the highest grade commercially available.

Preparation of Intestinal and Hepatic Microsomes. C57BL/6J mice (7-week-old male, 21–26 g, and female, 17–20 g), BALB/c, C3H/HeJ, DBA/2, ddY, and ICR mice (7-week-old male, 21–34 g), and Sprague-Dawley rats (7-week-old male, 220–240 g, and female, 140–160 g) were obtained from SLC Japan (Hamamatsu, Japan). Animals were housed in the institutional animal facility in a controlled environment (temperature $25 \pm 1°C$ and 12-h light/dark cycle) with access to food and water ad libitum. Animals were acclimatized for a week before use. Animal were maintained in accordance with the National Institutes of Health Guide for Animal Welfare of Japan, as approved by the Institutional Animal Care and Use Committee of Kanazawa University.

Pooled duodenal, jejunal, iliac, and colonic microsomes from five mice or rats were prepared according to the method of Emoto et al. (2000) with slight modifications. Briefly, duodenum, jejunum, ileum, and colon were divided, cut longitudinally, and then washed in ice-cold 1.15% KCl by gentle swirling. The intestine was suspended in 3 vol of ice-cold buffer A [50 mM Tris-HCl buffer (pH 7.4) containing 150 mM KCl, 20% (v/v) glycerol, 1 mM EDTA, 1 mM (p-amidinophenyl)methanesulfonyl fluoride, 1 mg/ml trypsin inhibitor, 10 μM leupeptin, 0.04 U/ml aprotinin, and 1 μM bestatin] and homogenized using a motor-driven Teflon-tipped pestle. The homogenate was centrifuged at 9000g at 4°C for 20 min, and then the supernatant was centrifuged at 105,000g at 4°C for 60 min. The microsomal pellets were resuspended in ice-cold buffer A.

Pooled hepatic microsomes from five mice or rats were prepared according to the method described by Emoto et al. (2000). Protein concentrations were determined according to the method of Lowry et al. (1951) using bovine serum albumin as the standard.

Enzyme Assays. A typical incubation mixture contained 50 mM Tris-HCl buffer (pH 7.4), 5 mM MgCl$_2$ (except propofol and TFP, 10 mM), 25 μg/ml alamethicin, UDPGA, microsomes, and a substrate. In the preliminary study, the concentration of UDPGA was confirmed to reach a plateau level for each UGT activity. Microsomes with alamethicin were placed on ice for 15 min. In the preliminary study, a change of preincubation time did not affect the UGT activities. The final concentration of methanol (estradiol and propofol) or ethanol (MPA) in the reaction mixture was <1.5% (v/v). As described by Uchaipichat et al. (2004), because methanol (>1%) decreased more than 20% of the UGT1A6 activity, the final concentrations of methanol for 4-MU and 4-NP O-glucuronidation were <0.75% and <0.5% (v/v), respectively. A portion of the sample was subjected to high-performance liquid chromatography. The flow rate was 1.0 ml/min.

Estradiol 3-O-glucuronidation was determined according to the method of Yoon et al. (2003) with slight modifications. In the preliminary study, the rate of this activity was linear with respect to the microsomal protein concentrations (<0.1 mg/ml in mice and <0.05 mg/ml in rats) and incubation time (<15

min in mice and <30 min in rats). Therefore, in both mice and rats, the concentrations of microsomal protein were 0.05 mg/ml, and the reaction mixture was incubated for 15 min. The concentrations of UDPGA were 3 (mice) and 7 mM (rats). The analytical column was a TSKgel ODS-80Ts (4.6 × 150 mm, 5 μm; TOSOH, Tokyo, Japan), and the mobile phase was acetonitrile-1 mM perchloric acid (25:75, v/v).

4-MU O-glucuronidation was determined according to the method of Uchai-pichat et al. (2004) with slight modifications. In the preliminary study, the rate of this activity was linear with respect to the microsomal protein concentrations (<0.2 mg/ml in mice and <0.1 mg/ml in rats) and incubation time (<30 min in mice and <15 min in rats). In the reaction mixture, the concentrations of microsomal protein were 0.1 (mice) and 0.05 mg/ml (rats). In both mice and rats, the concentration of UDPGA was 3 mM, and the reaction mixture was incubated for 15 min. The analytical column was a CAPCEL PAK C$_{18}$ UG120 (4.6 × 150 mm, 5 μm; Shiseido, Tokyo, Japan), and the mobile phase was methanol-50 mM potassium phosphate buffer, pH 4.5 (20:80, v/v).

4-NP O-glucuronidation was determined according to the method of Hanioka et al. (2001) with slight modifications. In the preliminary study, the rate of this activity was linear with respect to the microsomal protein concentrations (<0.2 mg/ml in both mice and rats) and incubation time (<30 min in mice and <15 min in rats). In the reaction mixture, the concentrations of microsomal protein were 0.1 (mice) and 0.05 mg/ml (rats). In both mice and rats, the concentration of UDPGA was 3 mM, and the reaction mixture was incubated for 15 min. The analytical column was a Mightysil RP-18 (4.6 × 150 mm, 5 μm; Kanto Chemical, Tokyo, Japan), and the mobile phase was methanol-50 mM potassium phosphate buffer, pH 6.5 (6:94, v/v).

Propofol O-glucuronidation was determined according to the method of Fujiwara et al. (2007) with slight modifications. In the preliminary study, the rate of this activity was linear with respect to the microsomal protein concentrations (<0.25 mg/ml in mice and <1.0 mg/ml in rats) and incubation time (<30 min in mice and <45 min in rats). In the reaction mixture, the concentrations of microsomal protein were 0.25 (mice) and 0.5 mg/ml (rats). In both mice and rats, the concentration of UDPGA was 5 mM, and the reaction mixture was incubated for 30 min (mice) and 45 min (rats). The analytical column was a Mightysil RP-18 (4.6 × 150 mm, 5 μm), and the mobile phase was acetonitrile-0.1% acetic acid (40:60, v/v).

MPA O-glucuronidation was determined according to the method of Picard et al. (2005). In the preliminary study, the rate of this activity was linear with respect to the microsomal protein concentrations (<0.2 mg/ml in mice and <0.5 mg/ml in rats) and incubation time (<45 min in mice and <60 min in rats). In the reaction mixture, the concentrations of microsomal protein were 0.1 (mice) and 0.2 mg/ml (rats) and the concentration of UDPGA was 7 (mice) and 3 mM (rats). The reaction mixture was incubated for 30 min. Carboxy-butoxy ether of mycophenolic acid (4.6 nmol) was added as an internal standard. The analytical column was an Inertsil ODS-3 (4.6 × 250 mm, 5 μm; GL Sciences, Tokyo, Japan), and the mobile phase was acetonitrile-0.1% phosphoric acid (30:70, v/v).

Morphine 3-O-glucuronidation was determined according to the method of Katoh et al. (2005) with slight modifications. In the preliminary study, the rate of this activity was linear with respect to the microsomal protein concentrations (<1.0 mg/ml in mice and <0.2 mg/ml in rats) and incubation time (<105 min in mice and <30 min in rats). In both mice and rats, the concentrations of UDPGA and microsomal protein were 10 mM and 0.2 mg/ml, respectively. The reaction mixture was incubated for 90 min (mice) and 30 min (rats). The analytical column was a Develosil C30-UG-5 (4.6 × 150 mm, 5 μm; Nomura Chemical, Aichi, Japan) and the mobile phase was 50 mM sodium dihydrogen phosphate.

TFP N-glucuronidation was determined according to the method of Uchai-pichat et al. (2006) with slight modifications. The concentrations of UDPGA and microsomal protein were 2.5 mM and 0.25 mg/ml, respectively. The reaction mixture was incubated for 30 min. The analytical column was an Inertsil ODS-3 (4.6 × 150 mm), and the mobile phase was acetonitrile-0.1% trifluoroacetic acid (30:70, v/v).

Kinetic Analyses. The kinetic studies were performed using pooled liver microsomes of C57BL/6J mouse, pooled duodenal microsomes of C57BL/6J mouse, pooled rat liver microsomes, and pooled rat duodenal microsomes. When the kinetic parameters were determined, the concentrations of estradiol, 4-MU, 4-NP, propofol, MPA, and morphine ranged from 5 to 150, 10 to 640,

TABLE 1

Kinetic parameters of UGT activities in liver microsomes from male and female mice and rats

TFP *N*-glucuronide was not detected in liver microsomes from male and female mice and rats.

Substrate	Species	Sex	K_m (S_{50})	V_{max}	K_{si}	CL_{int} (CL_{max})	n^a
			μM	nmol/min/mg protein	μM	μl/min/mg protein	
Estradiol	Mouse	M	17 ± 3^b	6.1 ± 0.3		179^c	2.3
		F	18 ± 2^b	6.6 ± 0.4		183^c	2.3
	Rat	M	16 ± 3^b	6.1 ± 0.4		193^c	1.8
		F	16 ± 2^b	7.1 ± 0.3		231^c	1.8
4-MU	Mouse	M	71 ± 8^b	214 ± 9		1975^c	1.2
		F	59 ± 3^b	159 ± 3		1436^c	1.5
	Rat	M	130 ± 11^b	264 ± 11		1146^c	1.4
		F	130 ± 6^b	286 ± 7		1241^c	1.3
4-NP	Mouse	M	116 ± 23	40 ± 2		341	
		F	112 ± 24	33 ± 2		293	
	Rat	M	378 ± 73	81 ± 7		213	
		F	635 ± 108	73 ± 6		115	
Propofol	Mouse	M	31 ± 3	1.9 ± 0.1	1069 ± 96	62	
		F	51 ± 11	2.5 ± 0.3	514 ± 105	49	
	Rat	M	16 ± 4	0.22 ± 0.07		14	
		F	51 ± 21	0.06 ± 0.01		1.2	
MPA	Mouse	M	307 ± 59	24 ± 2		78	
		F	242 ± 21	27 ± 1		111	
	Rat	M	344 ± 26	5.9 ± 0.2		17	
		F	304 ± 24	3.0 ± 0.1		9.9	
Morphine	Mouse	M	421 ± 17	19 ± 0		46	
		F	318 ± 15	20 ± 0		64	
	Rat	M	1406 ± 17	39 ± 0		27	
		F	1319 ± 79	35 ± 1		26	

[a] Hill coefficient.
[b] S_{50}.
[c] CL_{max}.

10 to 1000 (10 to 1500 in mouse duodenum), 5 to 2000, 10 to 1000, and 20 to 6000 μM, respectively. The kinetic parameters and S.E.s were estimated from the fitted curves using a computer program (KaleidaGraph; Synergy Software, Reading, PA) designed for nonlinear regression analysis. The following equations were used: Michaelis-Menten equation, $V = V_{max} \cdot [S]/(K_m + [S])$; Hill equation, $V = V_{max} \cdot [S]^n/(S_{50}{}^n + [S]^n)$; and substrate inhibition equation, $V = V_{max} \cdot [S]/(K_m + [S] + [S]^2/K_{si})$, where V is the velocity of the reaction, S is the substrate concentration, K_m is the Michaelis-Menten constant, V_{max} is the maximum velocity, S_{50} is the substrate concentration showing the half-V_{max}, n is the Hill coefficient, and K_{si} is the substrate inhibition constant. Intrinsic clearance (CL_{int}) was calculated as V_{max}/K_m for Michaelis-Menten kinetics. For sigmoidal kinetics, maximum clearance (CL_{max}) was calculated as $V_{max} \cdot (n - 1)/(S_{50} \cdot n(n - 1)^{1/n})$ to estimate the highest clearance (Houston and Kenworthy, 2000). In the present study, if the Hill coefficient was more than 1.2, the kinetic data were fit to the Hill equation.

UGT Activities in Intestine. The UGT activities were determined using pooled duodenal, jejunal, ileal, and colonic microsomes from C57BL/6J mice or rats. The concentrations of estradiol, 4-MU, 4-NP, propofol, MPA, and morphine were 20, 100, 300, 60, 200, and 200 μM, respectively, which were the concentrations below apparent K_m values in duodenal microsomes from mice or rats. Other experimental conditions were the same as described above. For investigation of strain differences in mice, the UGT activities were determined in pooled duodenal and liver microsomes from six strains using six substrates.

Results

Kinetic Analyses of UGT Activities in Mouse and Rat Liver Microsomes Using Seven UGT Substrates. To investigate species and sex differences, kinetic analyses of estradiol 3-*O*-, 4-MU *O*-, 4-NP *O*-, propofol *O*-, MPA *O*-, morphine 3-*O*-, and TFP *N*-glucuronidation were determined in liver microsomes from male mice, female mice, male rats, and female rats. When kinetic parameters were determined, the concentrations of estradiol, 4-MU, 4-NP, propofol, MPA, and morphine ranged from 5 to 150, 10 to 640, 10 to 1000, 5 to 2000, 10 to 1000, and 20 to 6000 μM, respectively. Kinetic

parameters are shown in Table 1. In all kinetic analyses, the *r* values for fitting to the kinetic model were more than 0.97. The estradiol 3-*O*-glucuronidation in all liver microsomes was fitted to the Hill equation. The Hill coefficient in both male and female mice (2.3) was higher than that in both male and female rats (1.8). The 4-MU *O*-glucuronidation in all liver microsomes was fitted to the Hill equation. Kinetic parameters were different between mice and rats. The 4-NP *O*-glucuronidation in all liver microsomes was fitted to the Michaelis-Menten kinetics. The propofol *O*-glucuronidation in male and female mouse liver microsomes was fitted to the substrate inhibition kinetics, whereas those in male and female rat liver microsomes were fitted to the Michaelis-Menten kinetics. The MPA *O*-glucuronidation in all liver microsomes was fitted to the Michaelis-Menten kinetics. In females, species differences in the apparent K_m and V_{max} values were observed as in males. The morphine 3-*O*-glucuronidation in all liver microsomes was fitted to the Michaelis-Menten kinetics. The TFP *N*-glucuronidation in male mouse and male rat liver microsomes was measured. However, this activity was not detected in either mice or rats.

Microsomal UGT Activities in Duodenum, Jejunum, Ileum, and Colon from Mice and Rats. UGT activities using six different substrates were measured in microsomes prepared from male and female mouse and rat duodenum, jejunum, ileum, and colon (Fig. 1). In male mice, 4-NP *O*- and morphine 3-*O*-glucuronidation in colon were higher than those in other parts of the intestine, whereas estradiol 3-*O*-, 4-MU *O*-, and propofol *O*-glucuronidation in duodenum were higher than those in other parts of the intestine. In male rats, the duodenum exhibited higher activities of 4-NP, propofol, MPA, and morphine glucuronidation than those in other parts of the intestine. In female rats, all UGT activities except morphine were decreased distally through the intestine. In all parts of the intestine, 4-MU *O*-, 4-NP *O*-, and morphine 3-*O*-glucuronidation in mice were lower than those in rats.
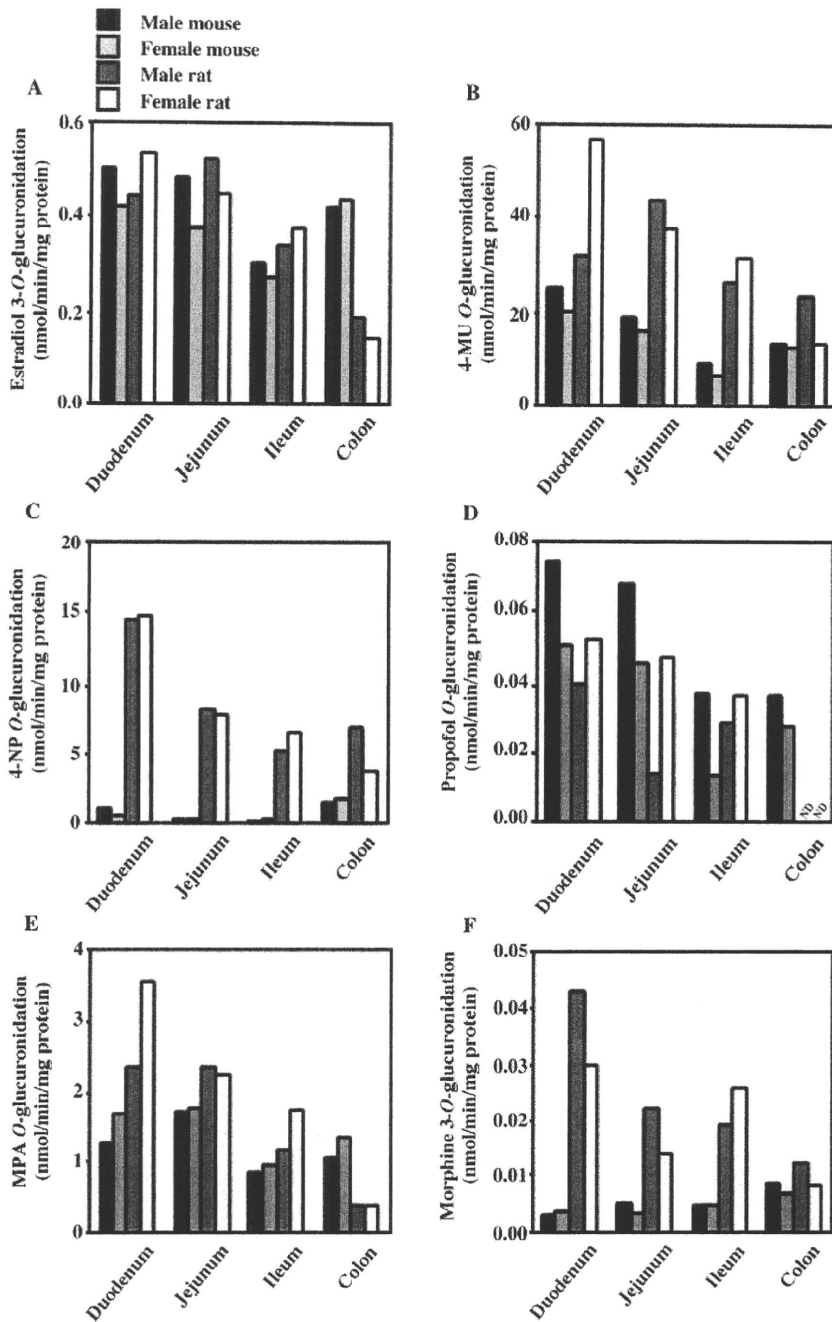
FIG. 1. UGT activities in duodenal, jejunal, ileal, and colonic microsomes from C57BL/6 mice and Sprague-Dawley rats. The formations of estradiol 3-*O*-glucuronide (A), 4-MU *O*-glucuronide (B), 4-NP *O*-glucuronide (C), propofol *O*-glucuronide (D), MPA *O*-glucuronide (E), and morphine 3-*O*-glucuronide (F) were determined as described under *Materials and Methods*. The concentrations of estradiol, 4-MU, 4-NP, propofol, MPA, and morphine were 20, 100, 300, 60, 200, and 200 μM, respectively. Each column represents the mean of duplicate determinations. ND, not detected.

Kinetic Analyses of UGT Activities in Duodenal Microsomes from Male Mice and Rats Using Seven UGT Substrates. Kinetic analyses of estradiol 3-*O*-, 4-MU *O*-, 4-NP *O*-, propofol *O*-, MPA *O*-, morphine 3-*O*-, and TFP *N*-glucuronidation in microsomes from male mice and rats were determined. Kinetic parameters are shown in Table 2. The estradiol 3-*O*-glucuronidation in duodenal microsomes from mice was fitted to the Hill equation. In comparison with liver, the CL_{max} values in duodenum were 6.5-fold lower. The Hill coefficient in duodenum was also lower than that in liver. On the other hand, this activity in rat duodenal microsomes was fitted to the Michaelis-Menten equation rather than to the Hill equation. When the kinetic data from rat duodenal microsomes were fit to the Hill equation, the S_{50} value, the V_{max} value, and the Hill coefficient were 29 μM, 1.2

nmol/min/mg protein, and 1.1, respectively. The 4-MU *O*-glucuronidation in duodenal microsomes from male mice and rats was fitted to the Michaelis-Menten equation. The 4-NP *O*-glucuronidation in duodenal microsomes from male mice did not reach a plateau level up to 1500 μM. In rat duodenal microsomes, this activity was fitted to the Michaelis-Menten kinetics with lower K_m values than in mice. The propofol *O*-glucuronidation in duodenal microsomes showed substrate inhibition at substrate concentrations >400 μM in male mice and >500 μM in female rats, but the plot did not fit to either the substrate inhibition kinetics or the two-site model used by Houston and Kenworthy (2000). Therefore, we did not calculate the kinetic parameters for propofol *O*-glucuronidation in duodenal microsomes. The MPA *O*-glucuronidation in duodenal microsomes from both male mice and rats was fitted to

TABLE 2

Kinetic parameters of UGT activities in duodenal microsomes from male mice and rats

TFP N-glucuronide was not detected in microsomes from male mice and rats.

Substrate	Species	K_m (S_{50})	V_{max}	CL_{int} (CL_{max})	n^a
		μM	nmol/min/mg protein	$\mu l/min/mg$ protein	
Estradiol	Mouse	42 ± 7^b	2.2 ± 0.2	28^c	1.6
	Rat	35 ± 10	1.3 ± 0.1	38	
4-MU	Mouse	164 ± 46	63 ± 7	387	
	Rat	416 ± 19	190 ± 4	458	
4-NP	Mouse	>1500			
	Rat	494 ± 117	33 ± 4	67	
MPA	Mouse	1272 ± 349	8.9 ± 1.6	7.0	
	Rat	340 ± 47	6.7 ± 0.4	20	
Morphine	Mouse	2380 ± 103	0.05 ± 0.00	0.02	
	Rat	320 ± 23	0.11 ± 0.00	0.34	

[a] Hill coefficient.
[b] S_{50}.
[c] CL_{max}.

the Michaelis-Menten kinetics. The CL_{int} value in mouse duodenum was 11-fold lower than that in liver. However, in rats, that value in duodenum (20 μl/min/mg protein) was similar to the value in liver (17 μl/min/mg protein). The morphine 3-O-glucuronidation in duodenal microsomes from both male mice and rats was fitted to the Michaelis-Menten kinetics. The CL_{int} value in mouse duodenum was lower than that in liver. The TFP N-glucuronidation in mouse and rat duodenal microsomes was determined. As in liver, these activities in both mice and rats were not detected.

Strain Differences of UGT Activities in Mouse Duodenal Microsomes. To investigate the strain differences in mice, the UGT activities using six UGT substrates were determined in duodenal microsomes from C57BL/6J, BALB/c, C3H/HeJ, DBA/2, ddY, and ICR mice (Fig. 2). For all UGT activities except 4-MU, C3H/HeJ mice showed the highest values among the six strains. The UGT activities in BALB/c and C3H/HeJ mice were relatively high compared with those in other mice. The UGT activities in the six strains showed a similar tendency between 4-NP O- and MPA O-glucuronidation or between estradiol 3-O- and propofol O-glucuronidation. The strain differences in UGT activities varied according to the substrates. Conversely, in liver, there was not much difference in UGT activities among the six mouse strains (Table 3).

Discussion

Information on species differences in UGT activities is insufficient. Intestine as well as liver plays an important role in xenobiotic metabolism. Numerous phase I and phase II drug-metabolizing enzymes are expressed in intestine. Recently, species differences in glucuronidation of the anti-human immunodeficiency virus drug bevirimat were reported (Wen et al., 2007). However, there have been no comprehensive analyses of UGT activities in intestine and liver from mice and rats. In the present study, kinetic analyses of UGT activities using seven typical substrates (estradiol, 4-MU, 4-NP, propofol, MPA, morphine, and TFP) in intestine and liver microsomes from mice and rats were investigated. In addition, strain differences in UGT activities in mouse duodenum were studied.

Estradiol 3-O-glucuronidation is catalyzed mainly by human UGT1A1. Rat UGT1A1 is responsible for this reaction (King et al., 1996). In human liver microsomes, estradiol 3-O-glucuronosyltransferase yielded an S_{50} value of 17 μM, and a Hill coefficient of 1.8 (Fisher et al., 2000a). The S_{50} value was almost the same among three species. In microsomes from humans, the estradiol 3-O-glucuronidation in small intestine was higher than that in liver as reported by Fisher et al. (2000b), which was contrary to the present results in mice

and rats. In the present study, the CL_{max} value for estradiol 3-O-glucuronidation in female rats was higher than that in male rats. For glucuronidation of bilirubin, another UGT1A1 substrate, sex differences in Wistar rats have been clarified (Muraca and Fevery, 1984). However, the sex differences in UGT1A1 activity are still unclear.

UGT1A6 is a major enzyme catalyzing the glucuronidation of various simple phenolic compounds such as 4-MU and 4-NP in the liver. UGT1A6 is likely to be functionally orthologous among several species including humans, rats, mice, and rabbits (Iyanagi et al., 1986; Harding et al., 1988; Lamb et al., 1994). The 4-MU glucuronidation in human liver microsomes followed the Michaelis-Menten kinetics (Miners et al., 1988) and was catalyzed by several human UGTs (Uchaipichat et al., 2004). The different kinetic models between humans and rodents might be due to the different UGT enzymes. In duodenum, the apparent K_m value for 4-NP glucuronidation in mice was higher than that in rats, suggesting that the affinity of 4-NP to mouse Ugt may be lower than that to rat UGT. In contrast, in liver, the apparent K_m value in mice was lower than that in rats. In the case of other UGT1A6 substrates, the hepatic serotonin O-glucuronidation in Wistar rats was higher than that in CD-1 mice (Krishnaswamy et al., 2003), whereas the hepatic acetaminophen O-glucuronidation in Wistar rats was lower than that in CD-1 mice (Court, 2001).

Rat *UGT1A9* is a pseudogene, but human *UGT1A9* and mouse *Ugt1a9* are not. The glucuronidation of propofol is catalyzed by human UGT1A8 (Mano et al., 2004) and by human UGT1A9 in the liver (Court, 2005) in a manner consistent with the substrate inhibition kinetics (Fujiwara et al., 2007). In the present study, the glucuronidation of propofol in liver microsomes from both male and female mice was fitted to the substrate inhibition kinetics, whereas those in other microsomes were not fit. These differences in the kinetic profile may be accounted for by the absence of UGT1A9 protein in rats. Propofol O-glucuronidation may be catalyzed by other UGTs, possibly UGT1A8, in rats.

MPA is the active metabolite of MMF, which induces gastrointestinal toxicity. Stern et al. (2007) reported that female rats were more susceptible to MMF-induced gastrointestinal toxicity than male rats, because of the fact that female rats showed lower intestinal MPA O-glucuronidation than male rats. In the present study, in duodenum the CL_{int} value for the MPA O-glucuronide formation in male mice was lower than that in male rats. This result suggests that male mice may be more susceptibility to MMF-induced gastrointestinal toxicity than male rats. Human UGT1A9 is mainly involved in hepatic MPA O-glucuronidation (Bernard and Guillemette, 2004). Picard et al. (2005) reported that in microsomes from humans the CL_{int} value in
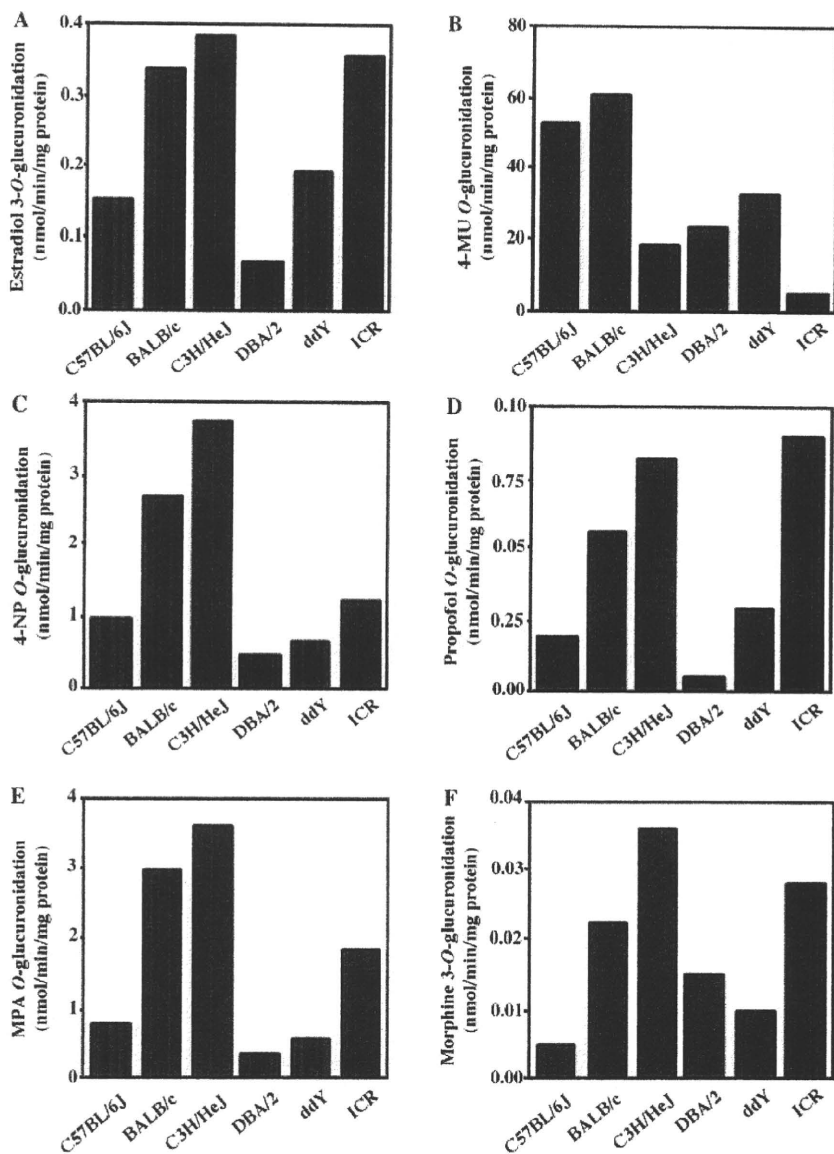
215

FIG. 2. UGT activities in duodenal microsomes from male C57BL/6J, BALB/c, C3H/HeJ, DBA/2, ddY, and ICR mice. The formations of estradiol 3-*O*-glucuronide (A), 4-MU *O*-glucuronide (B), 4-NP *O*-glucuronide (C), propofol *O*-glucuronide (D), MPA *O*-glucuronide (E), and morphine 3-*O*-glucuronide (F) were determined as described under *Materials and Methods*. The concentrations of estradiol, 4-MU, 4-NP, propofol, MPA, and morphine were 20, 100, 300, 60, 200, and 200 μM, respectively. Each column represents the mean of duplicate determinations.

TABLE 3

UGT activities in liver microsomes from the six mouse strains

Data represent the mean of duplicate determinations. The concentrations of estradiol, 4-MU, 4-NP, propofol, MPA, and morphine were 20, 100, 300, 60, 200, and 200 μM, respectively.

Strain	UGT Activities					
	Estradiol	4-MU	4-NP	Propofol	MPA	Morphine
	nmol/min/mg protein					
C57BL/6J	0.89	147	46	1.7	17	8.4
BALB/c	0.77	199	71	1.2	14	8.5
C3H/HeJ	0.79	169	62	1.7	17	8.4
DBA/2	0.82	133	56	3.5	28	8.2
ddY	0.80	160	63	3.5	25	8.3
ICR	0.71	136	65	3.3	26	8.6

liver (28.7 μl/min/mg protein) was higher than that in intestine (0.7 μl/min/mg protein). In the present study in mice, the CL_{int} value in liver was higher than that in duodenum, but mouse Ugt catalyzing MPA *O*-glucuronidation has not been determined yet. Rat UGT1A7 is mainly involved in MPA *O*-glucuronidation (Miles et al., 2005, 2006).

In the present study, the CL_{int} value in rats was similar in liver and duodenum and may be catalyzed by UGT1A7.

In humans, approximately 55% of morphine is metabolized into morphine 3-*O*-glucuronide and approximately 15% into morphine 6-*O*-glucuronide (Milne et al., 1996). The ratios of morphine 3-*O*-

glucuronide to morphine 6-*O*-glucuronide in liver microsomes of mice, rats, guinea pigs, and rabbits were 300:1, 90:1, 4:1, and 40:1, respectively (Kuo et al., 1991). The formation of morphine 3-*O*-glucuronide is catalyzed by human UGT2B7 (Turgeon et al., 2001) and rat UGT2B1 (King et al., 2000). However, there is no information on the mouse Ugt enzyme that catalyzes morphine 3-*O*-glucuronidation. Rat UGT2B1 and mouse Ugt2b1 are predominantly expressed in the liver (Shelby et al., 2003; Buckley and Klaassen, 2007). In the present study, the morphine 3-*O*-glucuronidation was higher in the liver, compared with intestine, in both mice and rats as well as humans (Fisher et al., 2000b). The indication is that the glucuronidation of morphine in mice may occur mainly in liver as in rats and humans. In addition, in the present study, there were no sex differences in morphine 3-*O*-glucuronidation in either mice or rats, consistent with a report on the sex differences in morphine glucuronidation in vivo and in vitro (Rush et al., 1983). However, in the case of bisphenol A glucuronidation catalyzed by rat UGT2B1, the ratio of bisphenol A glucuronide to total bisphenol A in liver microsomes was significantly higher (*P* = 0.015) in female than in male Wistar-Imamichi rats, and the relative hepatic expression level of UGT2B1 mRNA was significantly higher (*P* < 0.001) in female than in male rats (Takeuchi et al., 2004). Therefore, when morphine 3-*O*-glucuronidation in rat liver is evaluated, the involvement of other UGTs as well as UGT2B1 may need to be considered.

TFP is a specific probe substrate for human UGT1A4 (Uchaipichat et al., 2006). However, rat *UGT1A4* and mouse *Ugt1a4* are known to be pseudogenes. In the present study, TFP *N*-glucuronidation in mice and rats could not be detected. Therefore, we should be careful in studies of drugs catalyzed by UGT1A4.

In the present study, the UGT activities in mouse and rat duodenum, jejunum, ileum, and colon were determined. The UGT activities in rats tended to decrease from duodenum to ileum, whereas this tendency in mice differed according to the substrates. These phenomena may be due to the expression levels of UGT or to the function of the UGT, but further study is needed. Strassburg et al. (2000) reported that the UGT activities in human intestine were higher in the jejunum than in duodenum or ileum. The present study clarified that this tendency in intestine may be different among mice, rats, and humans.

There are few reports concerning strain differences in UGT activities in mice. The UGT activities of five different substrates, except for 4-MU, showed the highest activities in C3H/HeJ mice. In contrast, the glucuronidation in DBA/2 mice was relatively low compared with that in the other strains. The strain differences in estradiol 3-*O*-, 4-NP *O*-, propofol *O*-, and MPA *O*-glucuronidation were similar. Why such strain differences were observed is not known exactly.

In conclusion, the present study clarified the fact that species differences exist between rats and mice in terms of their duodenal and hepatic UGT activities. The species, strain, and sex differences may depend on the substrate or UGT enzyme. The present study will provide useful information for the selection of species for in vivo UGT studies. Furthermore, experimental animals are useful tools for the development of new drugs, and thus studies on species differences are of great value for extrapolating results from animals to humans. The present study will also provide useful information for predicting drug metabolism catalyzed by UGTs.

References

Bernard O and Guillemette C (2004) The main role of UGT1A9 in the hepatic metabolism of mycophenolic acid and the effects of naturally occurring variants. *Drug Metab Dispos* **32:**775–778.

Buckley DB and Klaassen CD (2007) Tissue- and gender-specific mRNA expression of UDP-glucuronosyltransferases (UGTs) in mice. *Drug Metab Dispos* **35:**121–127.
Burchell B, Soars M, Monaghan G, Cassidy A, Smith D, and Ethell B (2000) Drug-mediated toxicity caused by genetic deficiency of UDP-glucuronosyltransferases. *Toxicol Lett* **112–113:** 333–340.
Coffman BL, King CD, Rios GR, and Tephly TR (1998) The glucuronidation of opioids, other xenobiotics, and androgens by human UGT2B7Y(268) and UGT2B7H(268). *Drug Metab Dispos* **26:**73–77.
Court MH (2001) Acetaminophen UDP-glucuronosyltransferase in ferrets: species and gender differences, and sequence analysis of ferret UGT1A6. *J Vet Pharmacol Ther* **24:**415–422.
Court MH (2005) Isoform-selective probe substrates for in vitro studies of human UDP-glucuronosyltransferases. *Methods Enzymol* **400:**104–116.
Dutton GJ (1980) Acceptor substrates of UDP glucuronosyltransferase and their assay, in *Glucuronidation of Drugs and Other Compounds* (Dutton GJ ed) pp 69–78, CRC Press, Boca Raton, FL.
Emoto C, Yamazaki H, Shimada N, Nakajima M, and Yokoi T (2000) Characterization of cytochrome P450 enzyme involved in drug oxidations in mouse intestinal microsomes. *Xenobiotica* **10:**943–953.
Fisher MB, Campanale K, Ackermann BL, VandenBranden M, and Wrighton SA (2000a) In vitro glucuronidation using human liver microsomes and the pore-forming peptide alamethicin. *Drug Metab Dispos* **28:**560–566.
Fisher MB, Vandenbranden M, Findlay K, Burchell B, Thummel KE, Hall SD, and Wrighton SA (2000b) Tissue distribution and interindividual variation in human UDP-glucuronosyltransferase activity: relationship between UGT1A1 promoter genotype and variability in a liver bank. *Pharmacogenetics* **10:**727–739.
Fujiwara R, Nakajima M, Yamanaka H, Nakamura A, Katoh M, Ikushiro S, Sakaki T, and Yokoi T (2007) Effects of coexpression of UGT1A9 on enzymatic activities of human UGT1A isoforms. *Drug Metab Dispos* **35:**747–757.
Hanioka N, Jinno H, Tanaka-Kagawa T, Nishimura T, and Ando M (2001) Determination of UDP-glucuronosyltransferase UGT1A6 activity in human and rat liver microsomes by HPLC with UV detection. *J Pharm Biomed Anal* **25:**65–75.
Hanioka N, Takeda Y, Jinno H, Tanaka-Kagawa T, Naito S, Koeda A, Shimizu T, Nomura M, and Narimatsu S (2006) Functional characterization of human and cynomolgus monkey UDP-glucuronosyltransferase 1A6 enzymes. *Chem Biol Interact* **164:**136–145.
Harding D, Fournel-Gigleux S, Jackson MR, and Burchell B (1988) Cloning and substrate specificity of a human phenol UDP-glucuronosyltransferase expressed in COS-7 cells. *Proc Natl Acad Sci U S A* **85:**8381–8385.
Houston JB and Kenworthy KE (2000) In vitro-in vivo scaling of CYP kinetic data not consistent with the classical Michaelis-Menten model. *Drug Metab Dispos* **28:**246–254.
Iyanagi T, Haniu M, Sogawa K, Fujii-Kuriyama Y, Watanabe S, Shively JE, and Anan KF (1986) Cloning and characterization of cDNA encoding 3-methylcholanthrene inducible rat mRNA for UDP-glucuronosyltransferase. *J Biol Chem* **261:**15607–15614.
Katoh M, Matsui T, Okumura H, Nakajima M, Nishimura M, Naito S, Tateno C, Yoshizato K, and Yokoi T (2005) Expression of human phase II enzymes in chimeric mice with humanized liver. *Drug Metab Dispos* **33:**1333–1340.
King C, Finley B, and Franklin R (2000) The glucuronidation of morphine by dog liver microsomes: identification of morphine-6-*O*-glucuronide. *Drug Metab Dispos* **28:**661–663.
King CD, Green MD, Rios GR, Coffman BL, Owens IS, Bishop WP, and Tephly TR (1996) The glucuronidation of exogenous and endogenous compounds by stably expressed rat and human UDP-glucuronosyltransferase 1.1. *Arch Biochem Biophys* **332:**92–100.
Krishnaswamy S, Duan SX, Von Moltke LL, Greenblatt DJ, Sudmeier JL, Bachovchin WW, and Court MH (2003) Serotonin (5-hydroxytryptamine) glucuronidation in vitro: assay development, human liver microsome activities and species differences. *Xenobiotica* **33:**169–180.
Kuo CK, Hanioka N, Hoshikawa Y, Oguri K, and Yoshimura H (1991) Species difference of site-selective glucuronidation of morphine. *J Pharmacobiodyn* **14:**187–193.
Lamb JG, Straub P, and Tukey RH (1994) Cloning and characterization of cDNAs encoding mouse Ugt1.6 and rabbit UGT1.6: differential induction by 2,3,7,8-tetrachlorodibenzo-*p*-dioxin. *Biochemistry* **33:**10513–10520.
Lowry OH, Rosebrough NJ, Farr AL, and Randall RJ (1951) Protein measurement with the Folin phenol reagent. *J Biol Chem* **193:**265–275.
Mackenzie PI, Bock KW, Burchell B, Guillemette C, Ikushiro S, Iyanagi T, Miners JO, Owens IS, and Nebert DW (2005) Nomenclature update for the mammalian UDP glycosyltransferase (*UGT*) gene superfamily. *Pharmacogenet Genomics* **15:**677–685.
Mano Y, Usui T, and Kamimura H (2004) Effects of β-estradiol and propofol on the 4-methylumbelliferone glucuronidation in recombinant human UGT isozymes 1A1, 1A8 and 1A9. *Biopharm Drug Dispos* **25:**339–344.
Miles KK, Kessler FK, Smith PC, and Ritter JK (2006) Characterization of rat intestinal microsomal UDP-glucuronosyltransferase activity toward mycophenolic acid. *Drug Metab Dispos* **34:**1632–1639.
Miles KK, Stern ST, Smith PC, Kessler FK, Ali S, and Ritter JK (2005) An investigation of human and rat liver microsomal mycophenolic acid glucuronidation: evidence for a principal role of UGT1A enzymes and species differences in UGT1A specificity. *Drug Metab Dispos* **33:**1513–1520.
Milne RW, Nation RL, and Somogyi AA (1996) The disposition of morphine and its 3- and 6-glucuronide metabolites in humans and animals, and the importance of the metabolites to the pharmacological effects of morphine. *Drug Metab Rev* **28:**345–472.
Miners JO, Lillywhite KJ, Matthews AP, Jones ME, and Birkett DJ (1988) Kinetic and inhibitor studies of 4-methylumbelliferone and 1-naphthol glucuronidation in human liver microsomes. *Biochem Pharmacol* **37:**665–671.
Muraca M and Fevery J (1984) Influence of sex and sex steroids on bilirubin uridine diphosphate-glucuronosyltransferase activity of rat liver. *Gastroenterology* **87:**308–313.
Picard N, Ratanasavanh D, Prémaud A, Le Meur Y, and Marquet P (2005) Identification of the UDP-glucuronosyltransferase isoforms involved in mycophenolic acid phase II metabolism. *Drug Metab Dispos* **33:**139–146.
Rush GF, Newton JF, and Hook JB (1983) Sex differences in the excretion of glucuronide conjugates: the role of intrarenal glucuronidation. *J Pharmacol Exp Ther* **227:**658–662.
Shelby MK, Cherrington NJ, Vansell NR, and Klaassen CD (2003) Tissue mRNA expression of the rat UDP-glucuronosyltransferase gene family. *Drug Metab Dispos* **31:**326–333.
Sneyd JR, Simons PJ, and Wright B (1994) Use of proton NMR spectroscopy to measure propofol metabolites in the urine of the female Caucasian patient. *Xenobiotica* **24:**1021–1028.

Stern ST, Tallman MN, Miles KK, Ritter JK, Dupuis RE, and Smith PC (2007) Gender-related differences in mycophenolate mofetil-induced gastrointestinal toxicity in rats. *Drug Metab Dispos* **35:**449–454.

Strassburg CP, Kneip S, Topp J, Obermayer-Straub P, Barut A, Tukey RH, and Manns MP (2000) Polymorphic gene regulation and interindividual variation of UDP-glucuronosyltransferase activity in human small intestine. *J Biol Chem* **275:**36164–36171.

Takeuchi T, Tsutsumi O, Nakamura N, Ikezuki Y, Takai Y, Yano T, and Taketani Y (2004) Gender difference in serum bisphenol A levels may be caused by liver UDP-glucuronosyltransferase activity in rats. *Biochem Biophys Res Commun* **325:**549–554.

Tukey RH and Strassburg CP (2000) Human UDP-glucuronosyltransferases: metabolism, expression and disease. *Annu Rev Pharmacol Toxicol* **40:**581–616.

Turgeon D, Carrier JS, Lévesque E, Hum DW, and Belanger A (2001) Relative enzymatic activity, protein stability and tissue distribution of human steroid-metabolizing UGT2B subfamily members. *Endocrinology* **142:**778–787.

Uchaipichat V, Mackenzie PI, Elliot DJ, and Miners JO (2006) Selectivity of substrate (trifluoperazine) and inhibitor (amitriptyline, androsterone, canrenoic acid, hecogenin, phenylbutazone, quinidine, quinine, and sulfinpyrazone) "probes" for human UDP-glucuronosyltransferases. *Drug Metab Dispos* **34:**449–456.

Uchaipichat V, Mackenzie PI, Guo XH, Gardner-Stephen D, Galetin A, Houston JB, and Miners JO (2004) Human UDP-glucuronosyltransferases: isoform selectivity and kinetics of 4-methylumbelliferone and 1-naphthol glucuronidation, effects of organic solvents, and inhibition by diclofenac and probenecid. *Drug Metab Dispos* **32:**413–423.

Wen Z, Martin DE, Bullock P, Lee KH, and Smith PC (2007) Glucuronidation of anti-HIV drug candidate bevirimat: identification of human UDP-glucuronosyltransferases and species differences. *Drug Metab Dispos* **35:**440–448.

Yoon Y, Westerhoff P, Snyder SA, and Esparza M (2003) HPLC-fluorescence detection and adsorption of bisphenol A, 17β-estradiol, and 17α-ethynyl estradiol on powdered activated carbon. *Water Res* **37:**3530–3537.

Address correspondence to: Dr. Tsuyoshi Yokoi, Drug Metabolism and Toxicology, Division of Pharmaceutical Sciences, Graduate School of Medical Science, Kanazawa University, Kakuma-machi, Kanazawa 920-1192, Japan. E-mail: tyokoi@kenroku.kanazawa-u.ac.jp

Structure and characterization of human *carboxylesterase 1A1, 1A2,* and *1A3* genes

Tatsuki Fukami[a], Miki Nakajima[a], Taiga Maruichi[a], Shiori Takahashi[a], Masataka Takamiya[b], Yasuhiro Aoki[b], Howard L. McLeod[c] and Tsuyoshi Yokoi[a]

Objective Human *carboxylesterase (CES) 1A1* gene (14 exons) and *CES1A3* pseudogene (six exons) are inverted and duplicated genes in a reference sequence (NT_010498). In contrast, earlier studies reported the *CES1A2* gene (14 exons) instead of the *CES1A3* pseudogene. The sequences of the *CES1A2* gene downstream and upstream of intron 1 are identical with those of the *CES1A1* and *CES1A3* genes, respectively. A *CES1A1* variant of which exon 1 is converted with that of the *CES1A3* gene (the transcript is *CES1A2*) has recently been identified. We sought to clarify the confusing gene structure of human *CES1A*.

Methods A panel of 55 human liver as well as 318 blood samples (104 Caucasians, 107 African–Americans, and 107 Japanese) was used to clarify the gene structures of *CES1A1*, *CES1A2*, and *CES1A3*. Real-time reverse transcription-PCR and western blot analysis were carried out. Imidapril hydrolase activity in human liver microsomes and cytosol was determined by liquid chromatography-mass spectrometry (LC-MS)/MS.

Results By PCR analyses, we found that the *CES1A2* gene is a variant of the *CES1A3* gene. Four haplotypes, A (*CES1A1* wild type and *CES1A3*), B (*CES1A1* wild type and *CES1A2*), C (*CES1A1* variant and *CES1A3*), and D (*CES1A1* variant and *CES1A2*), were demonstrated. Ethnic differences were observed in allele frequencies of *CES1A1* variant (17.3% in Caucasians and African–Americans and 25.2% in Japanese) and *CES1A2* gene (14.4% in Caucasians, 5.1% in African–Americans, and 31.3% in Japanese). In human livers whose diplotype was A/A

and C/C or C/D, no CES1A2 and CES1A1 mRNA was detected, respectively. In the other participants, the CES1A1 mRNA levels were higher than the CES1A2 mRNA levels. The CES1A proteins translated from CES1A1 mRNA and CES1A2 mRNA were detected in both human liver microsomes and cytosol fractions suggesting that the differences in exon 1 encoding a signal peptide did not affect the subcellular localization. Imidapril hydrolase activities reflected the CES1A protein levels.

Conclusion We found that the *CES1A2* gene is a variant of the *CES1A3* pseudogene. The findings presented here significantly increase our understanding about the gene structure and expression properties of human CES1A. *Pharmacogenetics and Genomics* 18:911–920 © 2008 Wolters Kluwer Health | Lippincott Williams & Wilkins.

Introduction

Human carboxylesterases (CES) are members of the serine esterase superfamily and are responsible for hydrolysis of a wide variety of xenobiotic and endogenous compounds. In human, CES isoforms are classified into three families CES1, CES2, and CES3. CES1 is highly expressed in most organs including liver, but its expression in gastrointestinal tract is markedly low [1]. CES2 is expressed in extrahepatic tissues, especially in the gastrointestinal tract and at lower levels in the liver [2]. CES3 is expressed in the liver and gastrointestinal tract at extremely lower levels than CES1 and CES2 [3]. CES1 and CES2 are the most studied isozymes and have been

reported to be responsible for the biotransformation of a variety of clinically used drugs and prodrugs such as temocapril, imidapril, capecitabin, and irinotecan [4].

In human CES1 families, three isoforms, CES1A1, CES1A2, and CES1A3, have been identified. In a reference sequence (NT_010498), the *CES1A1* and *CES1A3* (earlier termed *CES4*) genes were inversely located on chromosome 16q13-q22.1 (Fig. 1) [5]. The *CES1A1* gene contains 14 exons spanning of about 30 kbp, whereas the *CES1A3* gene contains six exons spanning of about 14 kbp [6]. The *CES1A1* gene is functional, but *CES1A3* is a pseudogene because of a premature stop

Fig. 1
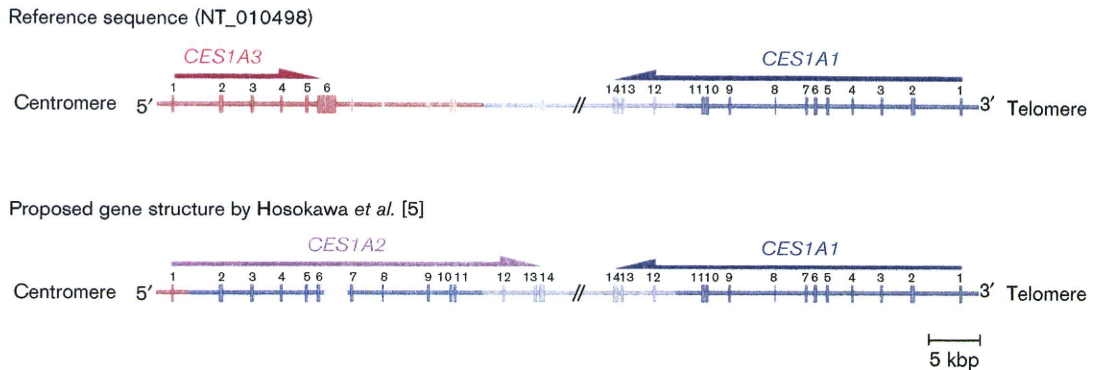
Schematic gene structure of human *carboxylesterase* (*CES*) *1A* from a DNA database (NT_010498) and that reported by Hosokawa *et al.* [5]. The *CES1A1* and *CES1A3* genes were inversely located on chromosome 16q13-q22.1. The CES1A1 gene contains 14 exons spanning of about 30 kbp, whereas the *CES1A3* gene contains six exons spanning of about 14 kbp. The blue and red regions represent the sequences specific for the *CES1A1* and *CES1A3* genes, respectively. In the *CES1A3* gene, sequences corresponding to exons 7–14 are found with high similarity to those of the *CES1A1* gene. The sequences downstream intron 11 of *CES1A1* and *CES1A3* are identical (purple region). The *CES1A2* gene also contains 14 exons spanning of about 30 kbp, and the sequences downstream of intron 1 are identical to those of the *CES1A1* gene, whereas the sequences upstream of intron 1 are identical to those of the *CES1A3* gene.

codon in exon 3. Interestingly, we noticed that there are sequences corresponding to exons 7–14 in the *CES1A3* gene, with high similarity to those of the *CES1A1* gene. Especially, the sequences downstream of intron 11 in the *CES1A3* gene are completely identical to those in the *CES1A1* gene. The finding is reminiscent of the fact that the *CES1A1* and *CES1A3* genes are inverse duplication genes.

In contrast, Hosokawa *et al.* [5] reported that the *CES1A1* and *CES1A2* genes are inversely located on chromosome 16q13-q22.1 (Fig. 1), although we could not access the original evidence. The *CES1A2* gene contains 14 exons spanning of about 30 kbp, and the sequences downstream of intron 1 are completely identical to those of the *CES1A1* gene. CES1A1 and CES1A2 have only four amino acid substitutions in their precursor protein sequences (encoded from exon 1), but mature proteins produced from both the *CES1A1* and *CES1A2* genes are identical, because exon 1 encodes a signal peptide (Table 1) [6–9]. We first noticed that the sequences upstream of intron 1 in the *CES1A2* gene are identical to those of the *CES1A3* gene. Taken together, the gene structure of human *CES1A* is uncertain and needs to be clarified.

Recently, Tanimoto *et al.* [7] have found a variant of the *CES1A1* gene (Fig. 2) in which exon 1 is converted with that of the *CES1A3* gene (also identical with *CES1A2*). The transcript from the *CES1A1* variant corresponds to CES1A2 mRNA (Table 1). It was presumed that the *CES1A2* gene might be another variant of the *CES1A1* gene. In this study, we sought to uncover the

Table 1 Gene, mRNA, precursor protein, and mature protein of human *CES1A*

| Gene	mRNA	Precursor protein	Mature protein	Reference
CES1A1	CES1A1	CES1A1	CES1A	Langmann *et al.* [6]
CES1A1 variant	CES1A2	CES1A2	CES1A	Tanimoto *et al.* [7]
CES1A2	CES1A2	CES1A2	CES1A	Shibata *et al.* [8]
CES1A3	CES1A3	–	–	Yan *et al.* [9]

CES, *carboxylesterase*.

gene structure of human *CES1A*. Thereafter, the inter-individual variability in the expression levels of CES1A1 and CES1A2 mRNA as well as CES1A protein was determined in relation to the gene structure.

Materials and methods
Chemicals and reagents
Taq polymerase, long and accurate (LA) Taq DNA polymerase, and blend TaqDNA polymerase were obtained from Greiner Japan (Tokyo, Japan), Takara (Shiga, Japan), and Toyobo (Tokyo, Japan), respectively. Restriction enzymes were purchased from New England BioLabs (Beverly, Maryland, USA) or Takara. Primers were commercially synthesized at Hokkaido System Sciences (Sapporo, Japan). RNAiso, the random hexamer and SYBR Premix Ex Taq were from Takara. RevaTra Ace (Mononey Murine Leukemia Virus Reverse Transcriptase RNaseH Minus) was from Toyobo. All other chemicals and solvents were of the highest grade commercially available.

Fig. 2
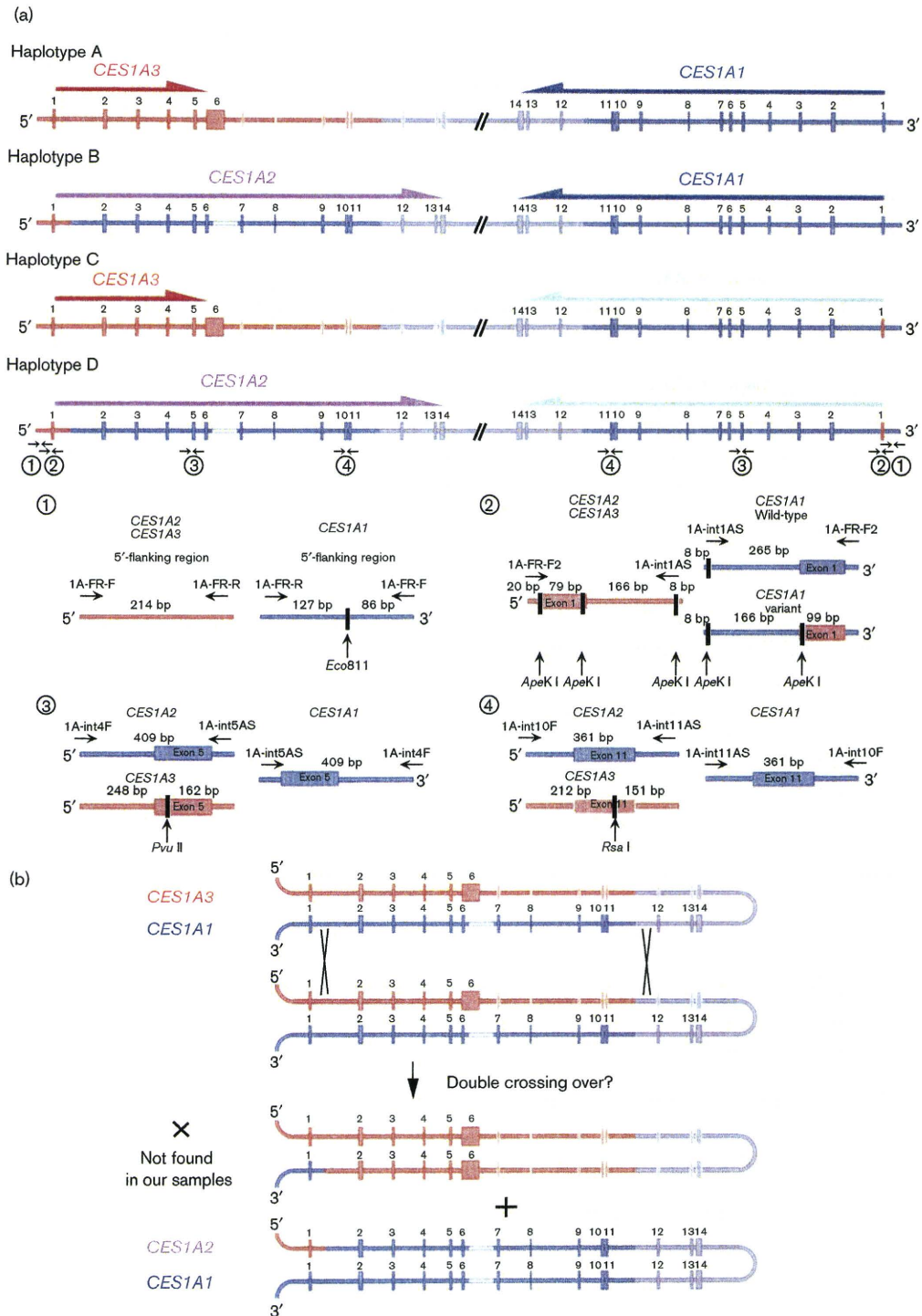
Possible haplotypes of the *carboxylesterase* (*CES*) *1A* genes and PCR-restriction fragment length polymorphism method to determine the diplotype as well as a proposed mechanism to create the *CES1A2* gene. (a) The reference sequence (NT_010498) and gene structure reported by Hosokawa *et al.* [5] are designated as haplotypes A and B, respectively. Likely, the gene structures with the *CES1A1* variants are designated as haplotypes C and D. PCR amplifications for the 5′-flanking region, exon 1, exon 5, and exon 11 were carried out with the primer sets indicated by horizontal arrows. Vertical arrows indicate the recognition sites of the restriction enzymes. The band intensities of the two fragments depicted with underlines for each PCR were quantified and corrected by the fragment lengths. (b) The *CES1A2* gene may be created by double crossing over between the *CES1A1* and *CES1A3* genes at intron 1 and downstream of intron 11. The assumed reciprocal product was not found in our samples.

Genomic DNA

Genomic DNA samples were extracted from 55 human livers and 318 human blood samples using a Puregene DNA isolation kit (Gentra Systems, Minneapolis, Minnesota, USA). Human liver samples from 17 donors (11 Caucasians, four Latino, one Black, and one Asian) were obtained from Human and Animal Bridging Research Organization (Chiba, Japan), and those from 38 Japanese were obtained from autopsy materials that were discarded after pathological investigation. The blood samples were from 104 Caucasian, 107 African–American, and 107 Japanese healthy participants who provided written informed consent. The use of the human livers and genomic DNA was approved by the Ethics Committees of Kanazawa University (Kanazawa, Japan) and Iwate Medical University (Morioka, Japan) as well as the Human Studies Committee of Washington University School of Medicine (St Louis, Missouri, USA).

Genotyping of carboxylesterase 1A1 variant

Allele specific-polymerase chain reaction (PCR) was established with a primer set of 1A1-FR-F and 1A1-ex1AS or 1A2/3-ex1AS (Table 2). The PCR mixture contained genomic DNA (100 ng), $1 \times$ PCR buffer [67 mmol/l Tris–HCl, pH 8.8, 16.6 mmol/l $(NH4)_2SO_4$, 0.45% Triton X-100, 0.02% gelatin], 1.5 mmol/l $MgCl_2$, 0.2 mmol/l deoxynucleotide-5'-triphosphates (dNTPs), 0.4 µmol/l each primer, and 0.5 U of Taq polymerase in a final volume of 25 µl. After an initial denaturation at 94°C for 3 min, the amplification was carried out by denaturation at 94°C for 25 s, annealing at 56°C for 25 s, and extension at 72°C for 30 s for 30 cycles, after a final extension at 72°C for 5 min. An aliquot (10 µl) of the PCR product (340 bp) was analyzed by electrophoresis with 2% agarose gel. The CES1A1 wild type was amplified with the primer set of 1A1-FR-F and 1A1-ex1AS and the CES1A1 variant was amplified with the primer set of 1A1-FR-F and 1A2/3-ex1AS.

Amplification of the carboxylesterase 1A2 or carboxylesterase 1A3 gene

To amplify the CES1A2 gene, LA-PCR was carried out to amplify the 5'-flanking region to exon 2 with the primer set 1A2/3-FR-F and 1A1/2-ex2AS (Table 2). The 1A2/3-FR-F primer anneals the CES1A2 and CES1A3 genes, whereas the 1A1/2-ex2AS primer anneals the CES1A1 and CES1A2 genes. Therefore, the primer set can specifically amplify the CES1A2 gene. The reaction mixture contained genomic DNA (200 ng), $1 \times$ LA-PCR buffer, 2.5 mmol/l $MgCl_2$, 0.4 mmol/l dNTPs, 0.4 µmol/l each primer, and 1 U of LA Taq DNA polymerase in a final volume of 25 µl. After an initial denaturation at 94°C for 1 min, the amplification was carried out by denaturation at 98°C for 20 s, annealing and extension at 68°C for 12 min (with prolongation for 15 s per 1 cycle during 13–26 cycles) for 26 cycles, after a final extension at 72°C for 10 min. An aliquot (10 µl) of the PCR product (3973 bp) was analyzed by electrophoresis with 0.8% agarose gel.

To amplify the CES1A3 gene, PCR was carried out to amplify intron 1 to exon 2 with the primer set 1A3-int1F and 1A3-ex2AS (Table 2), which specifically anneals the CES1A3 gene. The reaction mixture contained genomic DNA (200 ng), $1 \times$ PCR buffer, 2.5 mmol/l $MgCl_2$, 0.4 mmol/l dNTPs, 0.4 µmol/l each primer, and 1 U of Taq DNA polymerase in a final volume of 25 µl. After an initial denaturation at 94°C for 1 min, the amplification was carried out by denaturation at 94°C for 25 s, annealing at 55°C for 25 s, and extension at 72°C for 30 s for 30 cycles, after a final extension at 72°C for 5 min. An aliquot (10 µl) of the PCR product (380 bp) was analyzed by electrophoresis with 2.0% agarose gel.

Determination of diplotypes of carboxylesterase 1A genes

To investigate the diplotypes of the CES1A genes, a method to quantify the PCR products was applied as described in our earlier study [10]. PCR was carried out with quantified genomic DNA (100 ng) using the primer sets 1A-FR-F and 1A-FR-R (the 5'-flanking region), 1A-FR-F2 and 1A-int1AS (exon 1), 1A-int4F and 1A-int5AS (exon 5), and 1A-int10F and 1A-int11AS (exon 11), which can anneal all of the CES1A1, CES1A2, and CES1A3 genes (Table 2). The reaction mixture was the same as described above except for the primers. The reaction conditions were as follows: after an initial denaturation at 94°C for 3 min, the amplification was carried out by denaturation at 94°C for 25 s, annealing 58°C, 59°C, 55°C, and 60°C for 25 s for 5'-flanking region, exon 1, exon 5, and exon 11, respectively, and extension at 72°C for 30 s for 35 cycles, after a final extension at 72°C for 5 min. When the PCR product for the 5'-flanking region was digested with Eco81 I, the CES1A1 gene yields 127 and 86-bp fragments, and the CES1A2 and CES1A3 genes yield a 214-bp fragment (Fig. 2). These products (10 µl) were electrophoresed on a 3% agarose gel and visualized

Table 2 Primers used in this study

Primer	Sequence	Location
1A-FR-F	5'-GGTTAGAGTCCTGCAAGGGT-3'	5'-flanking region
1A-FR-R	5'-CTGCCAATTGCCTAATCCTCTAA-3'	5'-flanking region
1A1-FR-F	5'-CAAGGGTGAACCCTTATGTA-3'	5'-flanking region
1A2/3-FR-F	5'-CAAGGGTGACACCGTTATGCC-3'	5'-flanking region
1A-FR-F2	5'-GACAGCACAGTCCCTCTGA-3'	5'-flanking region
1A1-ex1F	5'-ATGTGGCTCCGTGCCT-3'	Exon 1
1A2/3-ex1F	5'-ATGTGGCTCCCTGCTC-3'	Exon 1
1A1-ex1AS	5'-AGAGAGTGGCCAGGATAAAG-3'	Exon 1
1A2/3-ex1AS	5'-CGAGAGTGGCCAGGACAAGA-3'	Exon 1
1A-int1AS	5'-CTCAGCTGCTCCAAGTCCAA-3'	Intron 1
1A1/2-int1AS	5'-GAGAACGTTCCCATGTCTTT-3'	Intron 1
1A3-int1F	5'-TTGCTCCTTAAACCAGCTTG-3'	Intron 1
1A1/2-ex2AS	5'-TCTTCACAAAGCTCCATGGT-3'	Exon 2
1A3-ex2AS	5'-TCTTCACAAAGTTCCATGGC-3'	Exon 2
1A-int4F	5'-GCTCAGTAAATAGTTGCCAGTT-3'	Intron 4
1A-int5AS	5'-TCTCATCAGCATCACATCAAG-3'	Intron 5
1A-int10F	5'-GGGGAGTTGCACAGGGCTT-3'	Intron 10
1A-int11AS	5'-GACCCTCAGCTGTTTCCATG-3'	Intron 11

by ethidium bromide staining. The intensities of the 127 (blue) and 214-bp (red) fragments were quantified using ImageQuant TL (GE Healthcare Science, Buckinghamshire, UK). When the PCR product for exon 1 was digested with *ApeK* I, the *CES1A1* wild type yields 265 and 8-bp fragments, the *CES1A1* variant yields 166, 99, and 8-bp fragments, and the *CES1A2* and *CES1A3* genes yield 166, 79, 20, and 8-bp fragments. These products (8 µl) were electrophoresed on a 2% agarose gel and visualized by ethidium bromide staining. The intensities of the 265 (blue) and 166-bp (red) fragments were quantified. When the PCR product for exon 5 was digested with *Pvu* II, the *CES1A1* and *CES1A2* genes yield a 409-bp fragment, and the *CES1A3* gene yields 248 and 162-bp fragments. These products (8 µl) were electrophoresed on a 2% agarose gel and visualized by ethidium bromide staining. The intensities of the 409 (blue) and 248-bp (red) fragments were quantified. When the PCR product for exon 11 was digested with *Rsa* I, the *CES1A1* and *CES1A2* genes yield a 361-bp fragment, and the *CES1A3* gene yields 212 and 151-bp fragments. These products (5 µl) were electrophoresed on a 3% agarose gel and visualized by ethidium bromide staining. The intensities of the 361 (blue) and 212-bp (red) fragments were quantified. The ratios of the intensities of the two bands (red/blue) corrected by the fragment lengths were calculated for each PCR reaction.

RNA preparation from human livers and real-time reverse transcription-PCR analyses

Total RNA samples were extracted from the human livers using RNAiso. The concentration and purity of RNA were determined spectrometrically. Complementary DNAs were synthesized as described earlier [11]. Real-time reverse transcription (RT)-PCR was carried out using the Smart Cycler (Cepheid, Sunnyvale, California, USA) for the quantifications of CEA1A1 and CES1A2 with the primer sets 1A1-ex1F and 1A1/2-ex2AS (Table 2) and 1A2/3-ex1F and 1A1/2-ex2AS, respectively as follows: a 1-µl portion of the RT mixture was added to a PCR mixture containing 0.4 µmol/l of each primer, 0.33 × SYBR Green I, 0.3 mmol/l dNTPs, 3 mmol/l $MgCl_2$, 1.25 U Ex-Taq HS and 1 × R-PCR buffer in a final volume of 25 µl. After an initial denaturation at 95°C for 30 s, the amplification was carried out by denaturation at 94°C for 4 s, annealing and extension at 64°C for 20 s for 45 cycles. Human glyceraldehyde-3-phosphate dehydrogenase mRNA was also quantified as described earlier [12]. The copy numbers were calculated using standard amplification curves.

Western blot analysis

Microsomes and cytosol fractions were prepared from 28 human livers as described earlier [13]. Microsomes (5 µg) and cytosol (10 µg) fractions were separated on 7.5% SDS-polyacrylamide gels and transferred onto polyvinylidene difluoride membrane, Immobilon-P

(Millipore, Billerica, Massachusetts, USA), and probed with rabbit anti-human CES1 polyclonal antibody (Abcam, Cambridge, Massachusetts, USA) at a dilution of 1:500. Biotinylated anti-rabbit IgG and a Vectastain avidin-biotin complex method kit (Vector Laboratories, Burlingame, California, USA) were used for diaminobenzidine staining. The quantitative analysis of the protein expression was carried out using ImageQuant TL Image Analysis software (GE Healthcare Science).

Enzyme assay

Imidapril hydrolase activity in human liver microsomes and cytosol fractions was determined as described earlier [14]. The substrate concentration was 20 µmol/l.

Results

Carboxylesterase 1A1 genotype and substitutive *carboxylesterase 1A2* and *carboxylesterase 1A3* genes

To investigate whether the *CES1A2* gene might be another variant allele of the *CES1A1* gene, in addition to the *CES1A1* variant allele identified by Tanimoto *et al.* [7], PCR was carried out to distinguish the *CES1A1* wild type, *CES1A1* variant, and *CES1A2* gene. Among 55 DNA samples, 37 samples were homozygotes of the wild type, and 15 and three samples were heterozygotes and homozygotes of the variant, respectively. The allele frequencies of the *CES1A1* wild type and variant were 80.9% and 19.1%, respectively. In 10 out of 15 samples genotyped as heterozygotes of the variant, the PCR product of the *CES1A2* gene (from the 5'-flanking region to exon 2) was detected, indicating that the *CES1A2* gene was not a variant allele of the *CES1A1* gene. Furthermore, PCR analyses revealed that, in 23 samples in which the *CES1A2* gene was absent, the *CES1A3* gene was present. In four samples in which the *CES1A3* gene was absent, the *CES1A2* gene was present. The other samples ($n = 28$) possessed both *CES1A2* and *CES1A3* genes. These results suggest that the *CES1A2* gene might be a variant of the *CES1A3* gene. The assumed mechanism by which the *CES1A2* gene was created is shown in Fig. 2b. The *CES1A2* gene might be created through double crossing over between the *CES1A3* and *CES1A1* genes at the intron 1 and downstream of intron 11 (Fig. 2b). If the *CES1A2* gene might be a variant of the *CES1A3* gene, four kinds of haplotypes, A, B, C, and D, are conceivable, by combination of the *CES1A1* wild type or variant (Fig. 2a). To evaluate this possibility, we next designed PCR-restriction fragment length polymorphism methods to determine the diplotypes of the *CES1A* gene.

Diplotype analyses of the *carboxylesterase 1A1* genes

Four primer sets were designed to amplify the *CES1A1* wild type, *CES1A1* variant, *CES1A2*, and *CES1A3* genes for the 5'-flanking region, exon 1, exon 5, and exon 11 (Fig. 2a). Digestion by the appropriate restriction enzymes could distinguish among these genes. The ratios of the intensities of the two bands (red/blue) corrected

223

by the fragment lengths were calculated for each PCR reaction. Collectively, 55 human liver samples were divided into eight groups (Fig. 3). We found 17 participants who had neither the *CES1A1* variant nor *CES1A2* (categorized in group I). Their diplotype was considered to be A/A. Hence, the ratios of the intensities of two bands (red/blue) at four regions were used as references; that is, the average of the ratios were defined as 1. The other 17 participants were categorized in group II. The ratios of the intensities of the two bands (red/blue) at the 5'-flanking region, exon 1, exon 5, and exon 11 were approximately 1.0, 1.0, 0.3, and 0.3, respectively, indicating that the diplotype was A/B. Likewise, the diplotype of the participants categorized in group III (*n* = 3) and group IV (*n* = 5) were determined to be B/B and A/C, respectively. The diplotype of the participants categorized in group V (*n* = 9) was determined to be either A/D or B/C, which could not be distinguished. The diplotype of the participants categorized in group VI (*n* = 1), group VII (*n* = 1), and group VIII (*n* = 2) were determined to be B/D, C/C, and C/D, respectively. Thus, it was clearly demonstrated that the *CES1A2* gene is a variant of the *CES1A3* gene. In 55 human liver samples, the diplotype D/D was not found. Among 55 samples, 23 were homozygotes of *CES1A3*, 28 were heterozygotes of *CES1A3/CES1A2*, and four were homozygotes of *CES1A2*, with the result that the allele frequencies of *CES1A3* and *CES1A2* were 67.3% and 32.7%, respectively. Interestingly, in 38 Japanese, the allele frequencies of *CES1A3* and *CES1A2* were 63.2% and 36.8%, respectively, whereas those in 11 Caucasians were 81.8% and 18.2%, respectively. To investigate the ethnic differences in the allele frequencies with a larger sample size, the diplotype analysis was applied for 104 Caucasian, 107 African–American, and 107 Japanese healthy participants (Table 3). Interestingly, a Japanese participant was genotyped as the diplotype D/D, categorizing in group IX. As summarized in Table 3, the frequencies of *CES1A1* variant in Caucasians, African–Americans, and Japanese were 17.3%, 17.3%, and 25.2%, respectively, and those of *CES1A2* were 14.4%, 5.1%, and 31.3%, respectively. Thus, the ethnic differences in the allele frequencies were demonstrated.

Expression levels of carboxylesterase 1A1 and carboxylesterase 1A2 mRNA in human liver samples

CES1A1 mRNA is transcribed from the *CES1A1* wild-type gene, whereas CES1A2 mRNA is transcribed from both the *CES1A1* variant and *CES1A2* genes. The expression levels of CES1A1 and CES1A2 mRNA in 55 human livers in eight groups were determined by real-time RT-PCR using the primer sets to amplify exon 1 to exon 2 of CES1A1 or CES1A2. CES1A1 mRNA was detected in the participants in groups I, II, and III who were homozygotes of the *CES1A1* wild type (Table 4). CES1A1 mRNA was also detected in the participants in groups IV, V, and VI who were heterozygotes of the

CES1A1 wild type/variant, but not in the participant in groups VII and VIII who were homozygotes of the *CES1A1* variant. In turn, CES1A2 mRNA was not detected in the participants in group I. Marginal levels of CES1A2 mRNA were, however, detected in groups II and III. By contrast, relatively high levels of CES1A2 mRNA were detected in the participants in groups IV, V, and IV who were heterozygotes of the *CES1A1* variant, as well as in those of groups VII and VIII who were homozygotes of the *CES1A1* variant. Thus, it was clearly demonstrated that the CES1A2 mRNA levels transcribed from the *CES1A2* gene were substantially lower than those transcribed from the *CES1A1* variant. In all participants in groups II, III, IV, V, and VI, the CES1A1 mRNA levels were higher than those of CES1A2 mRNA.

Carboxylesterase 1A protein level and enzyme activity in human liver microsomes and cytosol

As the signal peptide sequences of CES1A1 and CES1A2 are different, sequence differences might possibly change the subcellular localization of mature CES1A proteins derived from CES1A1 or CES1A2 precursors. To investigate this possibility, the mature CES1A protein levels in microsomes and cytosol fraction were determined in human liver samples expressing only CES1A1 mRNA (group I) or CES1A2 mRNA (groups VII and VIII). In nine samples in group I, CES1A protein was detected in both microsomes (1.00 ± 0.51 unit/mg) and cytosol (0.32 ± 0.20 unit/mg) fractions (Figs 4a, b). In three samples in groups VII and VIII, CES1A protein was detected in both microsomes (0.92 ± 0.24 unit/mg) and cytosol (0.07 ± 0.06 unit/mg) fractions. Thus, mature CES1A proteins derived from both CES1A1 and CES1A2 precursors likely localize both in endoplasmic reticulum (ER) and cytosol, although mature protein derived from the CES1A2 precursor was predominantly in ER. Imidapril hydrolase activities in human liver microsomes and cytosol reflected the CES1A protein levels (Fig. 4c).

Discussion

In this study, we found that the *CES1A2* gene is a variant of the *CES1A3* pseudogene. As a model, it was assumed that double crossing over might occur between the *CES1A1* and *CES1A3* genes at intron 1 and downstream of intron 11 (Fig. 2b). To investigate whether the reciprocal product gene exists or not, PCR analysis was carried out using a primer set of 1A1-ex1F and 1A3-ex2AS (Table 2) for 55 human liver samples. No samples, however, showed a detectable product (data not shown).

The sequence identity in the 5'-flanking region between the *CES1A1* and *CES1A2* genes is approximately 90%. Tanimoto *et al.* [7] have reported that the promoter activity of the *CES1A2* gene was significantly lower than that of the *CES1A1* gene by a luciferase assay using hepatoma cell line HepG2 and the esophageal squamous

Fig. 3
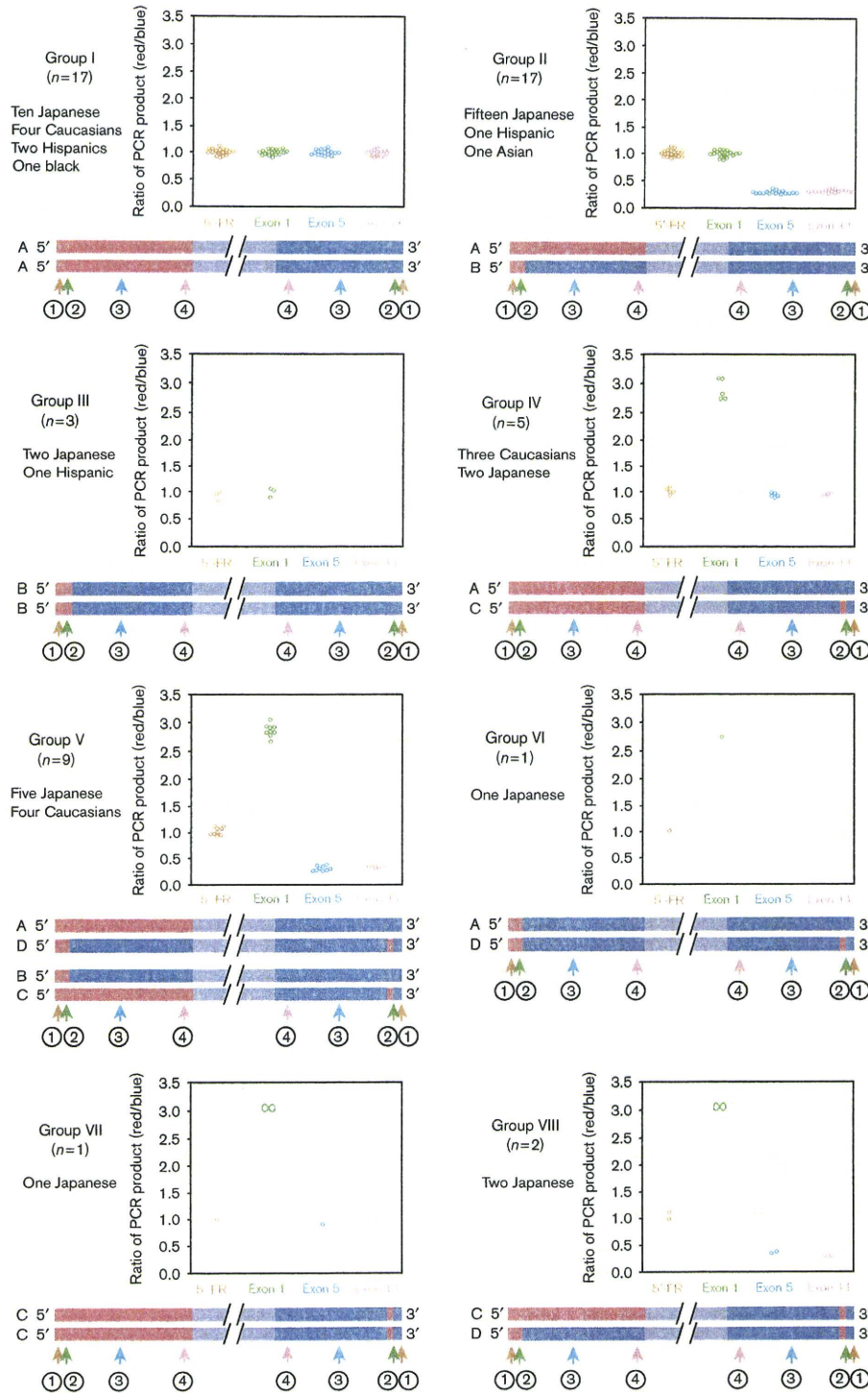
Determination of diplotype of *carboxylesterase* (*CES*) *1A* gene. Structures of haplotypes A, B, C, and D shown in Fig. 2a are simply depicted. The blue and red regions represent the sequences specific for the *CES1A1* and *CES1A3* genes, respectively. The purple region represents the common sequences. Vertical arrows with numbers indicate the amplified regions by PCR targeting the 5′-flanking region, exon 1, exon 5, and exon 11 shown in Fig. 2a. The ratios of the intensities of the two bands (red/blue) were calculated. The averages of the ratios at four regions in group I were defined as 1 because the diplotype was considered to be A/A. The ∞ means no detectable band from the blue region. Collectively, 55 samples were divided into eight groups, group I (diplotype A/A), group II (diplotype A/B), group III (diplotype B/B), group IV (diplotype A/C), group V (diplotype A/D or B/C), group VI (diplotype B/D), group VII (diplotype C/C), and group VIII (diplotype C/D).

Table 3 Diplotypes and allele frequencies of CES1A genes in Caucasians, African–Americans, and Japanese

Group	CES1A1 genotype	CES1A3 or CES1A2 genotype	Number of participants		
			Caucasians	African–Americans	Japanese
I	W/W	1A3/1A3	50	66	31
II	W/W	1A3/1A2	20	8	26
III	W/W	1A2/1A2	1	0	5
IV	W/V	1A3/1A3	22	27	12
V	W/V	1A3/1A2	8	2	21
VI	W/V	1A2/1A2	0	0	3
VII	V/V	1A3/1A3	3	3	6
VIII	V/V	1A3/1A2	0	1	2
IX	V/V	1A2/1A2	0	0	1
Total			104	107	107

Genotype	Frequency (%)		
CES1A1			
CES1A1 wild type	82.7	82.7	74.8
CES1A1 variant	17.3	17.3	25.2
CES1A3 or CES1A2			
CES1A3	85.6	94.9	68.7
CES1A2	14.4	5.1	31.3

CES, carboxylesterase; V, variant; W, wild type.

Table 4 CES1A1 and CES1A2 mRNA levels in human livers

| Group	Number of samples	CES1A1 genotype	CES1A3 or CES1A2 genotype	CES1A1/GAPDH mRNA (copy/0.1 µg)		CES1A2/GAPDH mRNA (copy/0.1 µg)	
				Mean±SD	Range	Mean±SD	Range
I	17	W/W	1A3/1A3	15.7±13.7	(2.1–52.9)	ND	
II	17	W/W	1A3/1A2	22.3±16.0	(4.2–61.7)	0.3±0.3	(0.0–0.8)
III	3	W/W	1A2/1A2	25.8±18.2	(10.0–45.7)	0.5±0.5	(0.0–1.2)
IV	5	W/V	1A3/1A3	16.0±12.1	(2.3–26.8)	8.2±7.0	(0.0–15.0)
V	9	W/V	1A3/1A2	7.9±7.8	(1.7–27.9)	4.8±4.8	(0.7–16.9)
VI	1	W/V	1A2/1A2	23.8		13.3	
VII	1	V/V	1A3/1A2	ND		5.3	
VIII	2	V/V	1A2/1A2	ND		5.6	(2.5–8.6)

CES, carboxylesterase; GAPDH, glyceraldehyde-3-phosphate dehydrogenase; ND, not detected; V, variant; W, wild type.

cell carcinoma cell line KYSE. In addition, Hosokawa et al. [15] recently reported that transcriptional factors Sp 1 and C/EBP could bind to the CES1A1 promoter region, but not to the CES1A2 promoter region by a luciferase assay using human hepatoma cell line FLC7 and Drosophila SL2 as well as a gel shift mobility assay. These results suggest that subtle differences in the sequences at the 5'-flanking region between CES1A1 and CES1A2 affect the transcriptional activity. Supporting their report, in our human liver samples, the levels of CES1A2 mRNA transcribed from the CES1A2 gene were substantially lower than those transcribed from the CES1A1 variant (Table 4). CES1A3 mRNA was not detected in the human liver samples (data not shown). Thus, it is conceivable that the CES1A3 promoter (identical with the CES1A2 promoter) might be hardly active in human livers. CES1A3 complementary DNA was originally cloned (named PCE-3) from human placenta [9]. Therefore, in some extrahepatic tissues such as placenta, small intestine, colon, kidney, and lung, the

levels of CES1A2 mRNA transcribed from the CES1A2 gene might not be lower than those transcribed from the CES1A1 variant. In the future, it will be interesting to determine the CES1A1 and CES1A2 mRNA levels as well as the CES1A protein levels and the subcellular localization in extrahepatic tissues, together with genotyping of the CES1A1 variant and CES1A2 or CES1A3 gene.

It has been reported that a single nucleotide polymorphism (SNP) in the 5'-flanking region of the CES1A2 gene, g.-861A > C, which was found in Japanese with 24.8% frequency, was associated with increased transcriptional activity and high responsiveness to imidapril [16]. In that report, the 5'-flanking regions of CES1A2 and CES1A3 were not distinguished. When we investigated our samples, out of 28 heterozygotes of CES1A2/CES1A3, the SNP was heterozygously detected in 13 participants and homozygously detected in one participant (data not shown) indicating that the SNP could be on both the CES1A2 and CES1A3 genes. To evaluate the clinical

226

Fig. 4
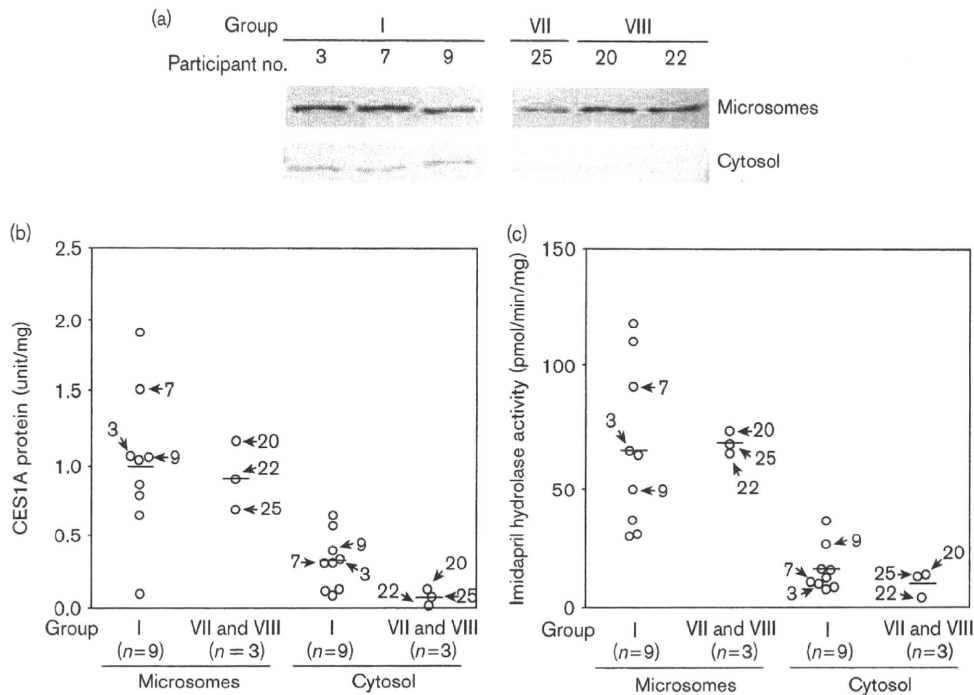
Carboxylesterase (CES) 1A protein levels and enzyme activity in human liver microsomes and cytosol. (a) Microsomes (5 µg) and cytosol (10 µg) fraction were separated by electrophoresis using 7.5% SDS-polyacrylamide gel. The CES1A protein was detected using rabbit anti-human *CES1A* antibody. Representative data for three out of nine samples in group I, one sample in group VII, and two samples in group VIII are shown. (b) The CES1A protein levels in group I ($n=9$) expressing only CES1A1 mRNA were compared with those in groups VII and VIII ($n=3$) expressing only CES1A2 mRNA. The average value of the CES1A protein levels in microsomes from group I was defined as 1 unit/mg. (c) Imidapril hydrolase activities in human liver microsomes and cytosol were determined by liquid chromatography-mass spectrometry (LC-MS/MS). The substrate concentration was 20 µmol/l. Horizontal bars show the average values in each group. The numbers with arrows show the sample numbers.

significance of the SNP, it should be determined whether the SNP was on the *CES1A2* or *CES1A3* gene because only the *CES1A2* gene encodes a functional enzyme.

Earlier studies reported that CES1A protein was mainly localized on the ER [17]. Our recent study, however, found that CES1A protein was also detected in cytosol fraction [18]. The CES1A protein purified from the human liver cytosol fraction had no signal peptide. The mechanisms regulating the subcellular localization of CES remain to be determined. Recently, Hosokawa [19] reported that no CES1A protein was detected in cytosol from human livers expressing only CES1A1 mRNA. In contrast to their report, in our western blot analysis a clear band was detected in cytosol from human livers expressing only CES1A1 mRNA (Figs 4a, b). We found that mature CES1A proteins derived from both CES1A1 and CES1A2 precursors were localized both in ER and cytosol, although the mature protein derived from the CES1A2 precursor was predominantly in the ER. The data of imidapril hydrolase activities in human liver microsomes and cytosol (Fig. 4c) supported the findings. Discordance between our and reported studies might

be because of differences in the antibodies used and sensitivity or the conditions of the western blot analysis. These results presented here suggested that the differences in exon 1 encoding a signal peptide between CES1A1 and CES1A2 did not affect the subcellular localization.

As shown in Table 4 and Fig. 4, CES1A mRNA, protein levels, and enzyme activity in human livers were highly variable. The regulation mechanisms of CES1A expression are not fully understood, but it is conceivable that CES1A might be induced in response to xenobiotics from the environment or diet and endobiotics, and likely other drug metabolizing enzymes such as cytochrome P450 and uridine diphosphate. Genetic polymorphisms in the 5′-flanking region of *CES1A* genes would contribute to interindividual differences in CES1A expression. Further studies are required to understand the cause of the interindividual differences of the CES1A expression.

In conclusion, we found that the *CES1A2* gene is a variant of the *CES1A3* gene. The levels of CES1A2 mRNA transcribed from the *CES1A2* gene were substantially

lower than those transcribed from the *CES1A1* variant. The findings presented here significantly increase our understanding about the gene structure and expression properties of human CES1A.

Acknowledgement

References

1 Imai T. Human carboxylesterase isozymes: catalytic properties and rational drug design. *Drug Metab Pharmacokinet* 2006; **21**:173–185.

2 Xu G, Zhang W, Ma MK, McLeod HL. Human carboxylesterase 2 is commonly expressed in tumor tissue and is correlated with activation of irinotecan. *Clin Cancer Res* 2002; **8**:2605–2611.

3 Sanghani SP, Quinney SK, Fredenburg TB, Davis WI, Murry DJ, Bosron WF. Hydrolysis of irinotecan and its oxidative metabolites, 7-ethyl-10-[4-N-(5-aminopentanoic acid)-1-piperidino] carbonyloxycamptothecin and 7-ethyl-10-[4-(1-piperidino)-1-amino]-carbonyloxycamptothecin, by human carboxylesterases CES1A1, CES2, and a newly expressed carboxylesterase isoenzyme, CES3. *Drug Metab Dispos* 2004; **32**:505–511.

4 Imai T, Taketani M, Shii M, Hosokawa M, Chiba K. Substrate specificity of carboxylesterase isoforms and their contribution to hydrolase activity in human liver and small intestine. *Drug Metab Dispos* 2006; **34**: 1734–1741.

5 Hosokawa M, Furihata T, Yaginuma Y, Yamamoto N, Koyano N, Fujii A, *et al.* Genomic structure and transcriptional regulation of the rat, mouse, and human carboxylesterase genes. *Drug Metab Rev* 2007; **39**:1–15.

6 Langmann T, Becker A, Aslanidis C, Notka F, Ullrich H, Schwer H, *et al.* Structural organization and characterization of the promoter region of a human carboxylesterase gene. *Biochim Biophys Acta* 1997; **1350**:65–74.

7 Tanimoto K, Kaneyasu M, Shimokuni T, Hiyama K, Nishiyama M. Human carboxylesterase 1A2 expressed from carboxylesterase 1A1 and 1A2 genes is a potent predictor of CPT-11 cytotoxicity *in vitro*. *Pharmacogenet Genomics* 2007; **17**:1–10.

8 Shibata F, Takagi Y, Kitajima M, Kubota Y, Omura T. Molecular cloning and characterization of a human carboxylesterase gene. *Genomics* 1993; **17**:76–82.

9 Yan B, Matoney L, Yang D. Human carboxylesterases in human placentae: enzymatic characterization, molecular cloning and evidence for the existence of multiple forms. *Placenta* 1999; **20**:599–607.

10 Fukami T, Nakajima M, Sakai H, McLead HL, Yokoi T. CYP2A7 polymorphic alleles confound the genotyping of CYP2A6*4A allele. *Pharmacogenomics J* 2006; **6**:401–412.

11 Nakajima M, Itoh M, Sakai H, Fukami T, Katoh M, Yamazaki H, *et al.* CYP2A13 expressed in human bladder metabolically activates 4-aminobiphenyl. *Int J Cancer* 2006; **119**:2520–2526.

12 Tsuchiya Y, Nakajima M, Kyo S, Kanaya T, Inoue M, Yokoi T. Human CYP1B1 is regulated by estradiol via estrogen receptor. *Cancer Res* 2004; **64**:3119–3125.

13 Tabata T, Katoh M, Tokudome S, Hosokawa M, Chiba K, Nakajima M, *et al.* Bioactivation of capecitabine in human liver: involvement of the cytosolic enzyme on 5′-deoxy-5-fluorocytidine formation. *Drug Metab Dispos* 2004; **32**:762–767.

14 Takahashi S, Katoh M, Saitoh T, Nakajima M, Yokoi T. Allosteric kinetics of human carboxylesterase 1: species differences and interindividual variability. *J Pharm Sci.* In press.

15 Hosokawa M, Furihata T, Yaginuma Y, Yamamoto N, Watanabe N, Tsukada E, *et al.* Structural organization and characterization of the regulatory element of the human carboxylesterase (CES1A1 and CES1A2) genes. *Drug Metab Pharmacokinet* 2008; **23**:73–84.

16 Geshi E, Kimura T, Yoshimura M, Suzuki H, Koba S, Sakai T, *et al.* A single nucleotide polymorphism in the carboxylesterase gene is associated with the responsiveness to imidapril medication and the promoter activity. *Hypertens Res* 2005; **28**:719–725.

17 Satoh T, Hosokawa M. The mammalian carboxylesterases: from molecules to functions. *Annu Rev Pharmacol Toxicol* 1998; **38**:257–288.

18 Tabata T, Katoh M, Tokudome S, Nakajima M, Yokoi T. Identification of the cytosolic carboxylesterase catalyzing the 5′-deoxy-5-fluorocytidine formation from capecitabine in human liver. *Drug Metab Dispos* 2004; **32**:1103–1110.

19 Hosokawa M. Structure and catalytic properties of carboxylesterase isozymes involved in metabolic activation of prodrugs. *Molecules* 2008; **13**:412–431.